Cell Reports

Article

A VQ-motif-containing protein fine-tunes rice immunity and growth by a hierarchical regulatory mechanism

Graphical abstract

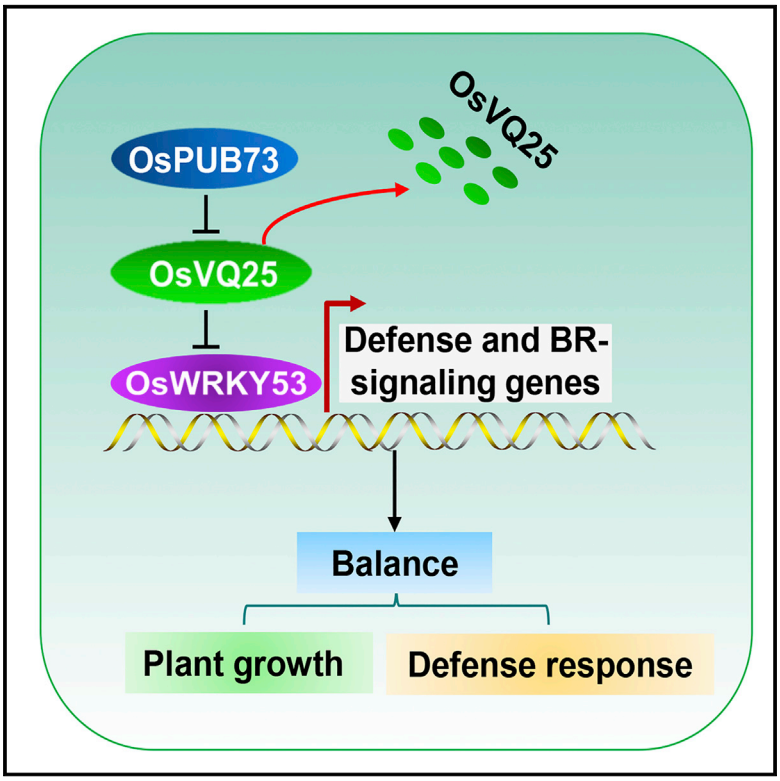

Authors

Zeyun Hao, Jinfu Tian, Hong Fang, ..., Guo-Liang Wang, Lanqin Xia, Yuese Ning

Correspondence

xialanqin@caas.cn (L.X.),
ningyuese@caas.cn (Y.N.)

In brief

Hao et al. show that loss-function of a VQ-motif-containing protein OsVQ25 confers broad-spectrum disease resistance. A U-box E3 ligase OsPUB73 interacts with and degrades OsVQ25, while OsVQ25 suppresses the transcriptional activity of a transcription factor OsWRKY53, highlighting that OsVQ25 balances plant immunity and growth by a hierarchical regulatory mechanism.

Highlights

- The U-box E3 ligase OsPUB73 positively regulates broad-spectrum disease resistance
- OsPUB73 interacts with and promotes the degradation of the VQ-motif protein OsVQ25
- The *osvq25* mutant confers broad-spectrum disease resistance without a growth penalty
- OsVQ25 interacts with and suppresses the transcriptional activity of OsWRKY53

Hao et al., 2022, Cell Reports *40*, 111235
August 16, 2022
https://doi.org/10.1016/j.celrep.2022.111235

CellPress

Cell Reports

CellPress
OPEN ACCESS

Article

A VQ-motif-containing protein fine-tunes rice immunity and growth by a hierarchical regulatory mechanism

Zeyun Hao,[1,8] Jinfu Tian,[2,8] Hong Fang,[1,3,8] Liang Fang,[1] Xiao Xu,[1] Feng He,[1] Shaoya Li,[2] Wenya Xie,[4] Qiang Du,[3] Xiaoman You,[1] Debao Wang,[1] Qiuhong Chen,[3] Ruyi Wang,[1] Shimin Zuo,[4] Meng Yuan,[5] Guo-Liang Wang,[6] Lanqin Xia,[2,7,*] and Yuese Ning[1,9,*]

[1]State Key Laboratory for Biology of Plant Diseases and Insect Pests, Institute of Plant Protection, Chinese Academy of Agricultural Sciences, Beijing 100193, China

[2]Institute of Crop Sciences, Chinese Academy of Agricultural Sciences, Beijing 100081, China

[3]College of Agronomy, Hunan Agricultural University, Changsha 410128, China

[4]Key Laboratory of Plant Functional Genomics of the Ministry of Education/ Jiangsu Key Laboratory of Crop Genomics and Molecular Breeding, Agricultural College of Yangzhou University, Yangzhou 225009, China

[5]National Key Laboratory of Crop Genetic Improvement, National Center of Plant Gene Research, Huazhong Agricultural University, Wuhan 430070, China

[6]Department of Plant Pathology, The Ohio State University, Columbus, OH 43210, USA

[7]Hainan Yazhou Bay Seed Laboratory/National Nanfan Research Institute (Sanya), Chinese Academy of Agricultural Sciences, Sanya 572024, China

[8]These authors contributed equally

[9]Lead contact

*Correspondence: xialanqin@caas.cn (L.X.), ningyuese@caas.cn (Y.N.)

https://doi.org/10.1016/j.celrep.2022.111235

SUMMARY

Rice blast and bacterial blight, caused by the fungus *Magnaporthe oryzae* and the bacterium *Xanthomonas oryzae* pv. *oryzae* (*Xoo*), respectively, are devastating diseases affecting rice. Here, we report that a rice valine-glutamine (VQ) motif-containing protein, OsVQ25, balances broad-spectrum disease resistance and plant growth by interacting with a U-Box E3 ligase, OsPUB73, and a transcription factor, OsWRKY53. We show that OsPUB73 positively regulates rice resistance against *M. oryzae* and *Xoo* by interacting with and promoting OsVQ25 degradation via the 26S proteasome pathway. Knockout mutants of *OsVQ25* exhibit enhanced resistance to both pathogens without a growth penalty. Furthermore, OsVQ25 interacts with and suppresses the transcriptional activity of OsWRKY53, a positive regulator of plant immunity. OsWRKY53 downstream defense-related genes and brassinosteroid signaling genes are upregulated in *osvq25* mutants. Our findings reveal a ubiquitin E3 ligase-VQ protein-transcription factor module that fine-tunes plant immunity and growth at the transcriptional and posttranslational levels.

INTRODUCTION

Plant diseases are caused by many different pathogens and can result in devastating yield losses in crop production (Nelson et al., 2018; Ning et al., 2017). Developing crop varieties with durable, broad-spectrum resistance (BSR) is the most economical and sustainable way to control diseases (Kou and Wang, 2010; Nelson et al., 2018). Among BSR types, species-non-specific (SNS) BSR confers resistance against two or more pathogens (Ke et al., 2017; Li et al., 2020). Because crops are often successively attacked by multiple pathogens during the growing season, SNS BSR provides better disease control than species-specific BSR (Ke et al., 2017). In rice, over 40 SNS BSR genes have been identified; they encode membrane-associated pattern recognition receptors, defense-signaling (DS) proteins, pathogenesis-related proteins, and susceptibility (S) proteins (Li et al., 2020). For example, the DS protein (IPA1) positively regulates SNS BSR to the blight bacterium *Xanthomonas oryzae* pv. *oryzae* (*Xoo*) and the rice blast fungus *Magnaporthe oryzae* (Liu et al., 2019; Wang et al., 2018). By contrast, the S gene *Bsr-k1* encoding an RNA-binding protein negatively regulates SNS BSR to *Xoo* and *M. oryzae* (Zhou et al., 2018). However, the functions of these proteins in SNS BSR and their potential underlying mechanisms in plants remain elusive.

The ubiquitin-proteasome system (UPS) plays critical roles in plant-microbe interactions and in immune responses to pathogens (Ning et al., 2016; Zeng et al., 2006). In the UPS, E3 ligases (E3s) are key factors that ubiquitinate target proteins and promote the degradation of some ubiquitinated proteins (Sadanandom et al., 2012). Depending on their structures, E3s are assigned to three categories: RING or U-box ligases, HECT ligases, and Cullin-RING ligases (Vierstra, 2009). Functions for

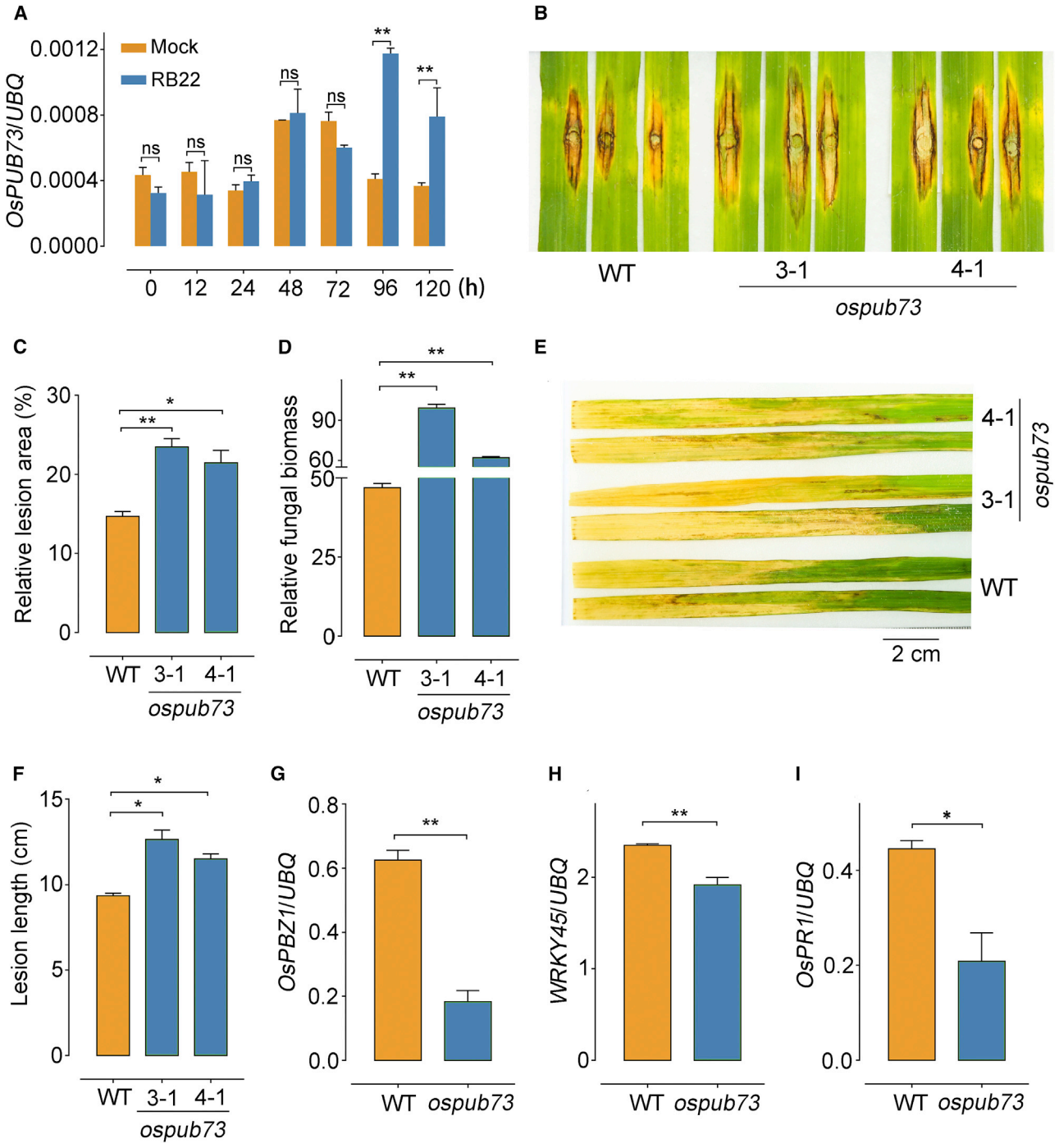

Figure 1. Expression pattern of *OsPUB73* and resistance phenotypes of the *ospub73* knockout mutant to *M. oryzae* and *Xoo*

(A) *OsPUB73* expression in Nipponbare (NPB) plants inoculated with the compatible *M. oryzae* isolate RB22, as determined by qRT-PCR. We used ddH_2O containing 0.1% (v/v) Tween 20 as the mock-inoculation control and rice *UBIQUITIN* (*UBQ*) as the reference gene to normalize gene expression. Values are means ± SEM of two biological replicates.

(B–D) Phenotypes of leaves from 8-week-old *ospub73* mutant plants inoculated with the compatible *M. oryzae* isolate RB22 (B), the percentage of leaf area with lesions, as measured by ImageJ (C), and relative fungal biomass, as determined by qPCR $[2^{[CT(OsUbq)-CT(MoPot2)]}]$ (D). Values are means ± SEM (n = 3 biological replicates).

(E and F) Phenotypes of leaves from 8-week-old *ospub73* mutant plants inoculated with the *Xoo* isolate PXO99A (E), and lesion length (F). Values are means ± SEM (n = 3 biological replicates).

(legend continued on next page)

E3s in rice SNS BSR have been reported. For instance, the U-box E3 ligase SPL11 negatively regulates programmed cell death (PCD) and defense against rice pathogens by degrading the Rho GTPase-activating protein SPIN6 and the S-domain receptor-like kinase SDS2 (Fan et al., 2018; Liu et al., 2015). The *spl11* mutant generates PCD symptoms in leaves and exhibits non-specific resistance to *Xoo* and *M. oryzae* (Zeng et al., 2004). The RING-type E3 ligase EBR1 negatively regulates PCD and defense against pathogens in rice by degrading OsBAG4, and the *ebr1* mutant demonstrates enhanced resistance to *Xoo* and *M. oryzae* (You et al., 2016). In addition, the Cullin-RING E3 ligase OsCUL3a negatively regulates PCD and immunity by degrading OsNPR1 in rice (Liu et al., 2017). *OsCUL3a* loss-of-function mutation promotes H_2O_2 accumulation in rice and shows enhanced resistance to *Xoo* and *M. oryzae* (Liu et al., 2017). All these rice E3s negatively regulate SNS BSR, while rice E3s that positively regulate SNS BSR have not been documented.

Valine-glutamine (VQ) proteins are an ancient protein family with the conserved VQ-motif structure FxxhVQxhTG (Jiang et al., 2018). VQ proteins are involved in plant defense. In *Arabidopsis* (*Arabidopsis thaliana*), *MKS1* (also named *VQ21*) overexpression confers increased resistance to *Pseudomonas syringae* pv. *tomato* DC3000 but greater susceptibility to *Botrytis cinerea* with severe growth penalties (Andreasson et al., 2005; Fiil and Petersen, 2011; Petersen et al., 2010). Differently, *SIB1* (also named *VQ23*) overexpression increases resistance to *Pseudomonas syringae* and *Botrytis cinerea* compared with wild-type (WT) plants. Importantly, *SIB1*-overexpression plants also display growth retardation (Lai et al., 2011; Xie et al., 2010). In addition, plants with reduced *JAV1* (also named *VQ22*) expression are more resistant to necrotrophic pathogens and herbivorous insects (Hu et al., 2013). These studies indicate that VQ proteins have various functions in plant immunity. However, only a few VQ proteins confer SNS BSR without a growth penalty.

In terms of signal transduction, VQ proteins always interact with WRKY transcription factors (TFs), which then regulate downstream responses (Chi et al., 2013; Jing and Lin, 2015). For example, JAV1 interacts with WRKY51 to negatively regulate the expression of jasmonic acid (JA) biosynthesis genes (Yan et al., 2018). The rice genome encodes around 40 VQ-motif-containing proteins (Jiang et al., 2018). Among them, *OsVQ13* positively regulates rice resistance to *Xoo* and affects rice grain size (Uji et al., 2019), while *OsVQ14* and *OsVQ32* function redundantly to positively regulate rice resistance to *Xoo* (Li et al., 2021). However, whether these or other *VQ* genes are involved in SNS BSR and associated signal transduction cascades needs further investigation.

Here, we report that OsVQ25 interacts with and is degraded by the U-box E3 ligase OsPUB73 via the 26S proteasome. Genetic analysis showed that OsPUB73 positively regulates SNS BSR against rice pathogens. OsVQ25 interacts with the positive immune regulator OsWRKY53 and suppresses its transcriptional activity to negatively regulate SNS BSR in rice. Importantly, we demonstrate that loss of *OsVQ25* function in rice results in SNS BSR against *M. oryzae* and *Xoo* without a growth penalty. Our study reveals that the OsPUB73-OsVQ25-OsWRKY53 module balances SNS BSR and plant growth at the transcriptional and posttranslational levels under a hierarchical regulatory mechanism.

RESULTS

OsPUB73 positively regulates rice resistance to *M. oryzae* and *Xoo*

OsPUB73 is a functional U-box E3 ligase, the expression of whose encoding gene is induced by *M. oryzae* infection in rice cultivar TP309 (Zeng et al., 2008). To further explore the contribution of OsPUB73 to blast resistance, we confirmed its expression pattern in Nipponbare (NPB) rice plants infected with the compatible *M. oryzae* isolate RB22. Quantitative reverse transcriptase PCR (qRT-PCR) analysis showed that *OsPUB73* is highly induced at 96 h post inoculation (Figure 1A). To determine OsPUB73 function in rice immunity, we generated *ospub73* knockout mutants by clustered regularly interspaced short palindromic repeats (CRISPR)-associated protein 9 (Cas9)-mediated genome editing. We selected two independent homozygous lines, 3-1 and 4-1 (in which a 1-bp insertion or a 20-bp deletion leads to early termination and a frameshift mutation, respectively) (Figures S1A and S1B). We used the punch inoculation method to assess the resistance of the *ospub73* mutants to the compatible *M. oryzae* isolate RB22. At 2 weeks after inoculation, the *ospub73* mutants had developed larger disease lesions than the WT (Figures 1B and 1C). The relative fungal biomass, as measured by quantitative PCR (qPCR), was higher in *ospub73* mutants than in the WT (Figure 1D), suggesting that *OsPUB73* positively regulates *M. oryzae* resistance. To assess if the loss of *OsPUB73* function affects resistance to other pathogens, we inoculated WT and the *ospub73* mutants with the *Xoo* compatible isolate PXO99A. At 2 weeks after inoculation, the *Xoo* disease lesions were longer on the *ospub73* mutants than on the WT (Figures 1E and 1F), indicating that *OsPUB73* also positively regulates *Xoo* resistance. We also measured the relative transcript levels of three defense-related genes, *OsPBZ1*, *WRKY45*, and *OsPR1*, in WT and the *ospub73* mutants by qRT-PCR. All three genes were significantly downregulated in the *ospub73* mutants compared with the WT (Figures 1G–1I). Together, these results demonstrated that *OsPUB73* positively regulates SNS BSR in rice.

The VQ-motif protein OsVQ25 interacts with OsPUB73

To investigate the molecular mechanism of OsPUB73 in rice resistance, we identified OsPUB73-interacting proteins using immunoprecipitation (IP) followed by liquid chromatography-tandem mass spectrometry (LC-MS/MS) assays in rice protoplasts. Among the candidate proteins obtained from the LC-MS data, a VQ-motif-containing protein (encoded by LOC_Os06g45570, annotated and designated as *OsVQ25*) caught our attention, as it is

(G–I) Relative expression levels of the defense-related genes *OsPBZ1* (G), *WRKY45* (H), and *OsPR1* (I) in *ospub73* mutants and WT plants, as determined by qRT-PCR. Values are means ± SEM (n = 3 biological replicates). For (A), (C)–(D), and (F)–(I), asterisks indicate statistical significance ("ns" indicates no statistical significance at $p > 0.05$, *$p \leq 0.05$, **$p \leq 0.01$, Student's t test). See also Figure S1.

mainly expressed in rice leaves and seedlings and is induced by *Xoo* and *M. oryzae* (Kim et al., 2013; Li et al., 2014). We tested the interaction between OsVQ25 and OsPUB73 by a luciferase complementation imaging (LCI) assay in *Nicotiana benthamiana* leaves. Co-infiltration of *OsPUB73-Nluc* and *Cluc-OsVQ25* constructs led to a stronger luciferase reporter signal and higher luciferase activity than in the control combinations (Figures 2A and S2). We also performed a bimolecular fluorescence complementation (BiFC) assay in *N. benthamiana* leaves. Pairwise expression of constructs encoding the N-terminal part of the yellow fluorescent protein (YFP) fused to OsVQ25 (YN-OsVQ25) and of the C-terminal part of YFP fused to OsPUB73 (YC-OsPUB73) resulted in a YFP fluorescence signal in the cytoplasm and the nucleus at 72 h post infiltration, but not with the control combinations encoding YN-OsVQ25/YC and YN/YC-OsPUB73 (Figure 2B), indicating that OsVQ25 interacts with OsPUB73 in the cytoplasm and the nucleus. To explore the OsVQ25-OsPUB73 interaction *in vivo*, we performed a co-immunoprecipitation (Co-IP) assay by transiently expressing *OsVQ25-GFP* with *OsPUB73-HA* in rice protoplasts, using *NLuc-HA* and 2×*GFP* (two tandemly repeated *Green fluorescent protein* [*GFP*] genes) as negative controls. Immunoblot analysis with an anti-GFP antibody showed that OsVQ25-GFP co-precipitates with OsPUB73-HA, but not with the control NLuc-HA; in addition, 2×GFP did not co-precipitate with OsPUB73-HA (Figure 2C). Together, these results demonstrate that OsVQ25 interacts with the U-box E3 ligase OsPUB73 *in planta*.

OsVQ25 is degraded by OsPUB73 via the ubiquitin 26S proteasome

OsPUB73 possesses E3 ubiquitin ligase activity (Zeng et al., 2008). The interaction between OsVQ25 and OsPUB73 suggested that OsPUB73 might promote OsVQ25 degradation via ubiquitination. To test this idea, we generated a construct encoding OsPUB73-C, which is a truncated OsPUB73 variant with the C terminus of OsPUB73 but lacking the U-box domain, for a degradation assay. We co-transfected *OsVQ25-GFP* and *OsPUB73-HA* or *OsPUB73-C-HA* in rice protoplasts, using *NLuc-HA* as the control. OsVQ25-GFP abundance was comparable when *OsVQ25-GFP* was co-expressed with *NLuc-HA* or *OsPUB73-C-HA*. However, the intensity of the OsVQ25-GFP band was clearly weaker when *OsVQ25-GFP* was co-expressed with full-length *OsPUB73-HA* (Figure 2D, lane 2). We then asked if OsVQ25 degradation is affected by the proteasome inhibitor MG132. Accordingly, we treated rice protoplasts transfected with the *OsPUB73-HA* and *OsVQ25-GFP* plasmids with MG132, which revealed that MG132 inhibits OsVQ25-GFP degradation (Figure 2D, lane 4). ACTIN, the internal control, displayed a similar accumulation in all tested combinations, and the relative *OsVQ25* and *ACTIN* transcript levels were also similar (Figure 2D). These results suggest that OsPUB73 specifically promotes OsVQ25 degradation via the 26S proteasome-dependent pathway *in planta*.

The rice *osvq25* mutant exhibits enhanced resistance against *M. oryzae* and *Xoo*

OsVQ25 expression is induced by *M. oryzae* in rice cultivar CO39 (Li et al., 2014). To determine if *OsVQ25* participates in disease resistance, we confirmed its expression pattern in NPB plants infected with the compatible *M. oryzae* isolate RB22. *OsVQ25* was rapidly induced at 12 h and was highly expressed at 96 and 120 h post inoculation compared with mock-inoculated plants (Figure 3A). To explore the function of OsVQ25 in resistance, we generated *osvq25* knockout mutants by CRISPR-Cas9-mediated gene editing. After genotyping, we selected three independent homozygous mutant lines (28-1, 29-1, and 48-1; with a 1-bp insertion of an A, a C, and a T, respectively, all causing frameshift mutations) for punch inoculation assays (Figures S3A and S3B). Two weeks after inoculation with the compatible *M. oryzae* isolate RB22, *osvq25* mutants developed smaller disease lesions and accumulated less fungal biomass than the WT (Figures 3B–3D). Because *OsVQ25* is also induced by *Xoo* (Kim et al., 2013; Li et al., 2014), we inoculated *osvq25* mutants and the WT with the *Xoo* isolate PXO99A and observed that all three mutant lines are also more resistant to *Xoo* (Figures 3E and 3F). To verify that the *osvq25* mutants have SNS BSR, we inoculated the mutants with another compatible *M. oryzae* strain, RO1-1, and another compatible *Xoo* strain, PXO86. The *osvq25* mutants also showed enhanced resistance to these pathogen strains (Figures S3C–S3F). Consistent with the disease-resistant phenotypes of the mutants, expression of the defense-related genes *OsPBZ1*, *WRKY45*, and *OsPR1* was significantly higher in *osvq25* mutant plants than in WT plants (Figures 3G–3I). Together, these results demonstrate that *OsVQ25* negatively regulates SNS BSR in rice.

The enhanced disease resistance of the *osvq25* mutant does not affect major agronomic traits

To test if the enhanced resistance of the *osvq25* mutants affects rice growth, we assessed key agronomic traits in the WT and the mutants under field conditions. Both plant architecture and panicle type were similar in the *osvq25* mutants and WT plants (Figure 4A). The yield-related traits (effective tiller number, thousand-grain weight, spike length, spikelet number, plant height, and kernel number per spike) were also similar across the genotypes (Figures 4B–4G). In addition, grain length and grain width were almost the same in *osvq25* and WT plants (Figure 4H). These results indicate that the loss of OsVQ25 function does not incur a growth penalty in rice, and that *OsVQ25* is a valuable candidate gene for breeding SNS BSR rice varieties by genome editing.

OsVQ25 interacts with the transcription factor OsWRKY53 and suppresses its transcriptional activity

To further dissect the underlying mechanism of OsVQ25 function in rice disease resistance, we queried the STRING database (https://string-db.org) for potential OsVQ25-interacting proteins. We focused on one such protein, the transcription factor OsWRKY53. We used LCI assays to investigate their potential physical interaction in *N. benthamiana* leaves infiltrated with *CLuc-OsVQ25* and *OsWRKY53-NLuc* constructs. Indeed, we detected strong luminescence signal when *CLuc-OsVQ25* and *OsWRKY53-NLuc* were co-infiltrated, but not with any of the control combinations (Figure 5A). We also established that the interaction between OsVQ25 and OsWRKY53 is specific, as LCI assays with an unrelated WRKY family member, WRKY45, yielded luminescence signals as low as those of the negative

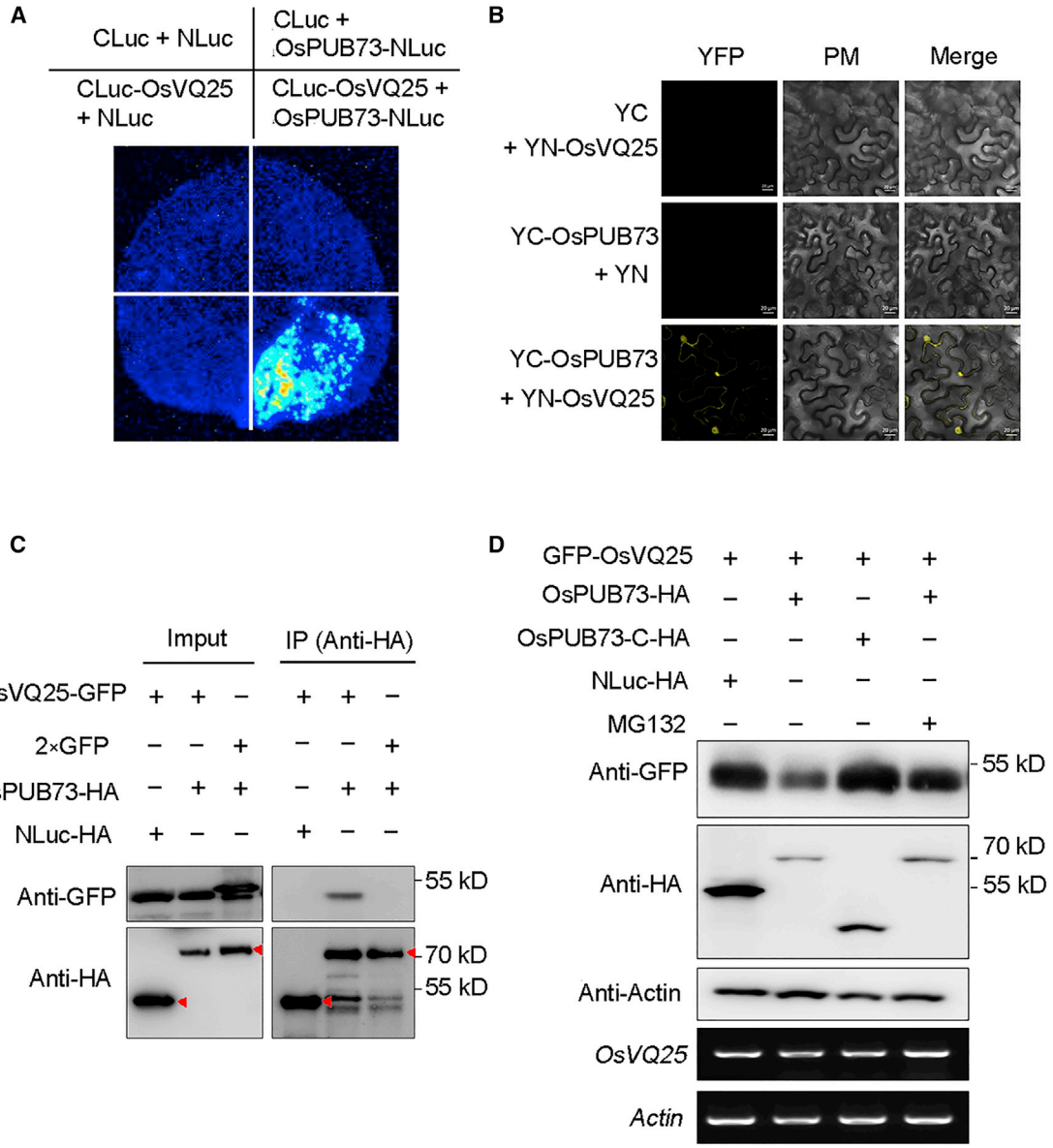

Figure 2. OsPUB73 interacts with and promotes the degradation of OsVQ25

(A) LCI assay showing the interaction between OsVQ25 and OsPUB73 in *N. benthamiana* leaves. Luminescence level was determined at 48 h after infiltration with the indicated constructs.

(B) BiFC assay to test the interaction between OsVQ25 and OsPUB73 in *N. benthamiana* leaves. Fluorescence from *N. benthamiana* leaf cells was acquired on a confocal microscope at 48 h after infiltration with the indicated constructs. Scale bar, 20 μm.

(C) Co-IP assay to test the interaction between OsVQ25 and OsPUB73 in transfected rice protoplasts. Total protein from rice protoplasts transfected with the indicated plasmid combinations was extracted and subjected to immunoprecipitation with anti-HA antibody. Red arrowheads indicate the expected proteins. There were three biological replicates with similar results.

(D) Degradation of OsVQ25 by OsPUB73 via the 26S proteasome pathway. *OsVQ25-GFP* was co-transfected with *OsPUB73-HA*, *OsPUB73-C-HA*, or *NLuc-HA* in rice protoplasts, followed by immunoblotting. ACTIN serves as an internal control. We added 20 μM MG132 or an equivalent volume of DMSO (as a control) at 12 h before sampling. The relative transcript levels of *OsVQ25* and *ACTIN* were detected by RT-PCR. There were three biological replicates with similar results.

controls (Figure S4A). We also performed BiFC in *N. benthamiana* leaves by co-infiltrating the *YN-OsVQ25* and *YC-OsWRKY53* constructs, which reconstituted YFP fluorescence in the nucleus, unlike the co-infiltration of *YN*-OsVQ25 and *YC-WRKY45*, which produced no detectable fluorescence (Figure 5B), indicating that OsVQ25 specifically interacts with OsWRKY53 in the nucleus. We also performed a Co-IP assay by transiently transfecting rice protoplasts with the *OsVQ25-GFP* and *OsWRKY53-HA* constructs. OsVQ25-GFP co-precipitated with OsWRKY53-HA when *OsVQ25-GFP* was co-transfected with *OsWRKY53-HA*

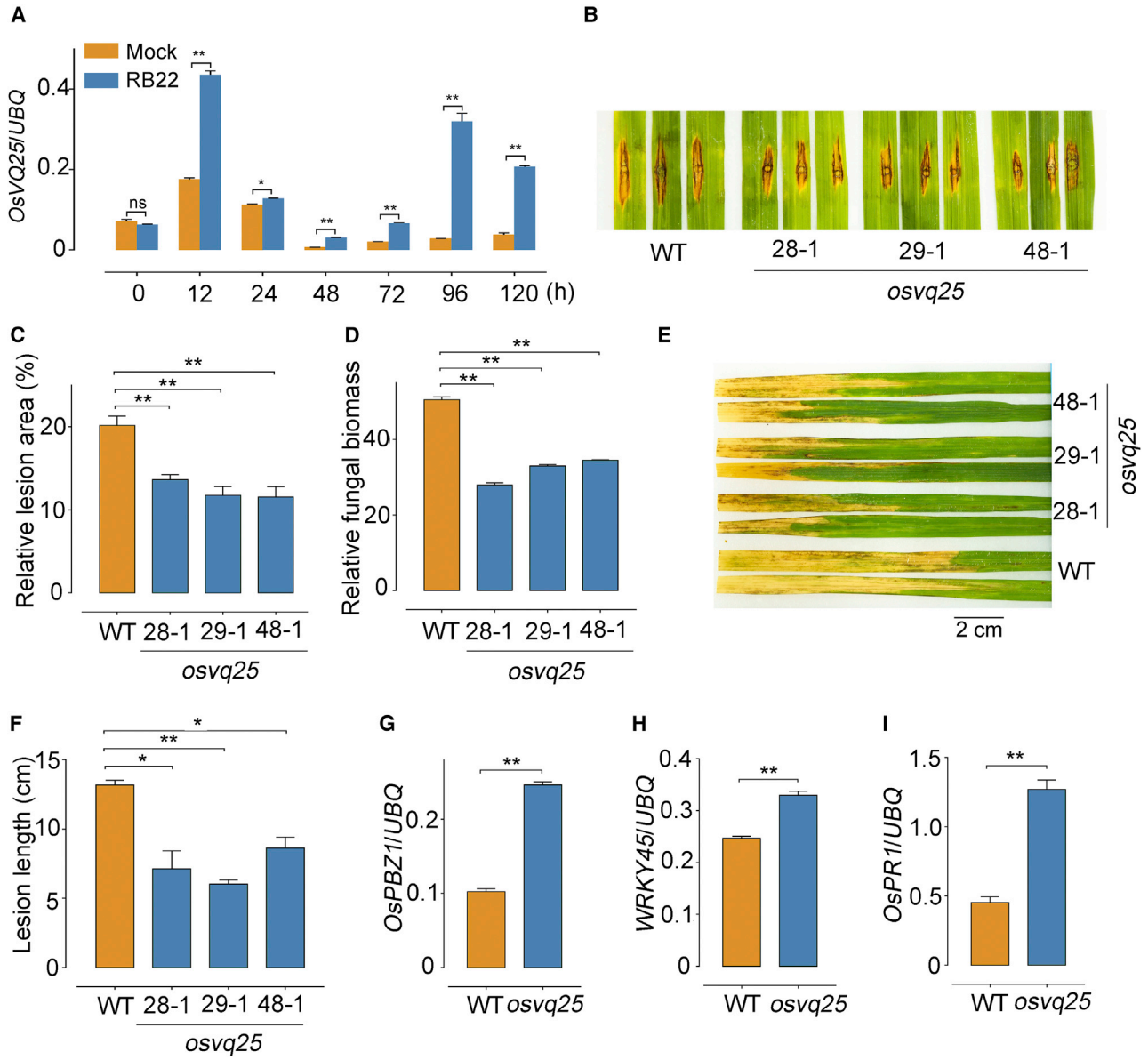

Figure 3. Expression pattern of *OsVQ25* and enhanced resistance of the *osvq25* mutant to *M. oryzae* and *Xoo*

(A) *OsVQ25* expression in NPB plants inoculated with the compatible *M. oryzae* isolate RB22, as determined by qRT-PCR. We used ddH_2O containing 0.1% (v/v) Tween 20 as the mock-inoculation control and rice *UBIQUITIN* (UBQ) as the reference gene to normalize gene expression. Values are means ± SEM (n = 2 biological replicates).

(B–D) Phenotypes of the leaves from 8-week-old *osvq25* mutant plants inoculated with the compatible *M. oryzae* isolate RB22 (B), percentage of leaf area with lesions, as measured by ImageJ (C), and relative fungal biomass, as determined by qPCR [$2^{[CT(OsUbq)-CT(MoPot2)]}$] (D). Values are means ± SEM (n = 3 biological replicates). Phenotypes of *osvq25* mutants inoculated with another compatible *M. oryzae* isolate, RO1-1.

(E and F) Phenotypes of the leaves of 8-week-old *osvq25* mutant plants inoculated with the *Xoo* isolate PXO99A (E), and lesion length (F). Values are means ± SEM (n = 3 biological replicates).

(G–I) Relative transcript levels of the defense-related genes *OsPBZ1* (G), *WRKY45* (H), and *OsPR1* (I) in *osvq25* mutants and WT plants as determined by qRT-PCR. Values are means ± SEM (n = 3 biological replicates). For (A), (C)–(D), and (F)–(I), asterisks indicate statistical significance ("ns" indicates no statistical significance at $p > 0.05$, *$p \leq 0.05$, **$p \leq 0.01$, Student's t test). See also Figure S3.

but not with the negative controls *NLuc-HA* or *WRKY45-HA*. The 2×GFP protein also did not co-precipitate with OsWRKY53-HA (Figure 5C). These results indicate that OsVQ25 interacts with OsWRKY53 *in planta*.

OsWRKY53-overexpressing rice plants have increased resistance to *M. oryzae* (Chujo et al., 2007, 2014). We investigated if *OsWRKY53* is involved in *M. oryzae* resistance by analyzing its expression pattern during *M. oryzae* infection: we observed that

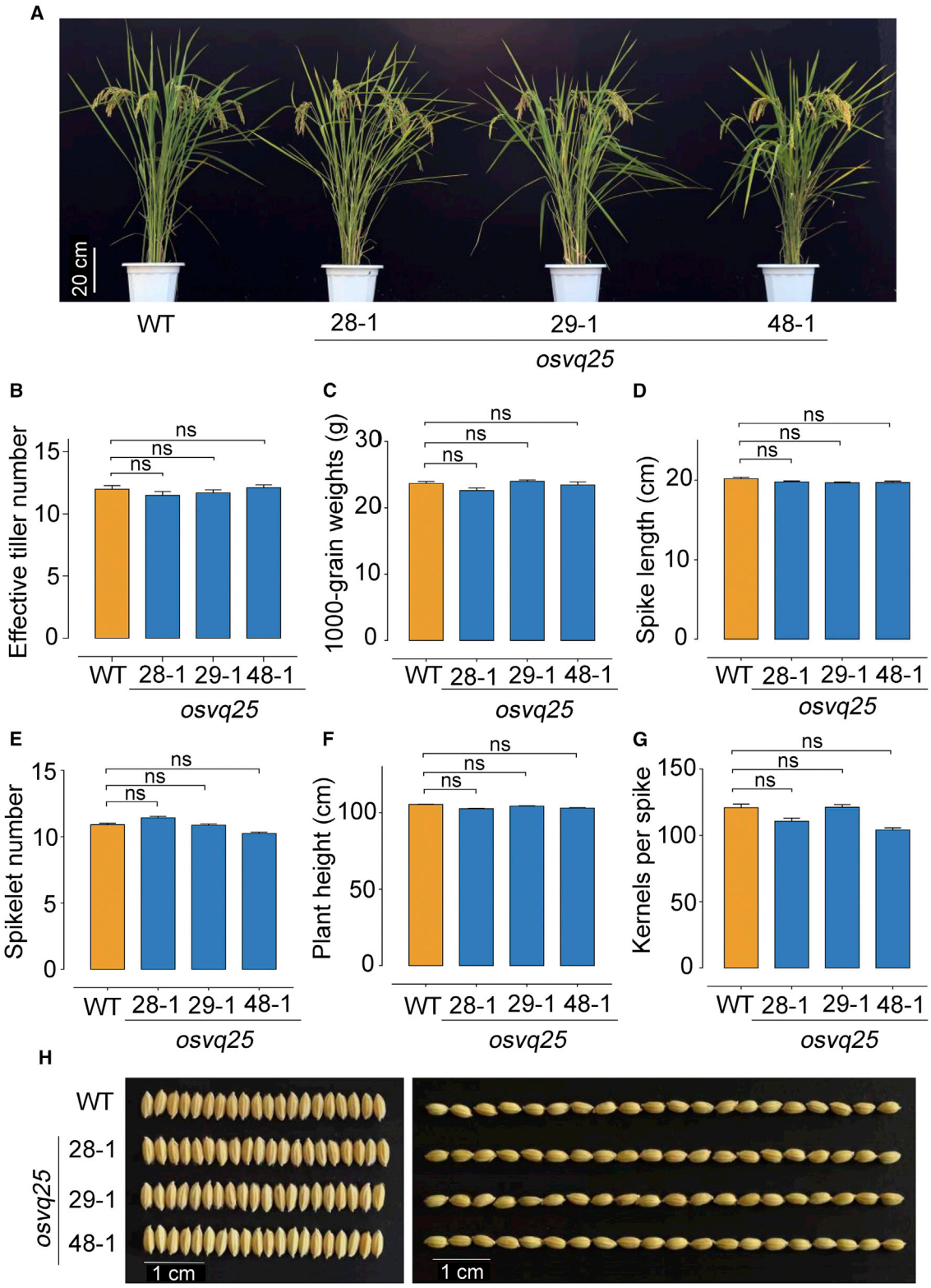

(legend on next page)

OsWRKY53 is highly induced at 12 h post inoculation (Figure S5A). To explore the role of OsWRKY53 in basal defense against *M. oryzae*, we used a previously generated *oswrky53* mutant in the Zhonghua11 (ZH11) background for punch inoculation (Xie et al., 2021). The *oswrky53* mutant exhibited decreased resistance to *M. oryzae* compared with ZH11 (Figures S5B and S5C), suggesting a positive role in the *M. oryzae* response. Next, we compared *OsWRKY53* expression in *osvq25* mutants and the WT. The *OsVQ25* knockouts did not affect *OsWRKY53* transcript levels (Figure S4B); furthermore, *OsWRKY53* expression was similar between *ospub73* and WT plants (Figure S4C). We then asked if OsVQ25 affects OsWRKY53 transcriptional activity in *Arabidopsis* protoplasts. Transcriptional activator AUXIN RESPONSE FACTOR 5 MIDDLE REGION (ARF5M) was used as a positive effector control (Wang et al., 2021). To this end, we cloned *OsWRKY53* coding sequences in-frame and downstream of the sequence of GAL4 DNA-binding domain, and we used a reporter construct consisting of the β-*glucuronidase* (*GUS*) reporter gene under the control of the GAL4(4X)-D1-3(4X) (Four copies of the GAL4 DNA-binding site fused immediately upstream of four tandem copies of the constitutive D1-3 element). The *OsWRKY53* effector construct showed a significantly higher relative GUS activity (normalized to firefly luciferase [LUC] activity) than that obtained with the *ARF5M* effector or the empty effector vector. However, relative GUS activity decreased significantly when we co-transfected the *OsWRKY53* effector construct with a construct expressing *OsVQ25*, but not with the control vector (Figures 5D and 5E). These results revealed that OsVQ25 reduces the transcriptional activity of OsWRKY53. Previous study reported that OsWRKY53 directly binds to the *OsMYB63* promoter *in vitro* and *in vivo*, and it represses *OsMYB63* transcription (Xie et al., 2021). To test if OsVQ25 inhibits OsWRKY53 DNA binding, we performed an electrophoretic mobility shift assay (EMSA) and a dual-luciferase assay, which both demonstrated that OsVQ25 impairs OsWRKY53 binding to the *OsMYB63* promoter (Figures S4D–S4F). We measured the expression levels of the defense genes *Chitinase* (Os01g0687400) and *PR-5* (Os12g0629700) in the *osvq25* mutants, as they are downstream of OsWRKY53 and are upregulated in *OsWRKY53*-overexpression plants (Chujo et al., 2014). The expression of these genes was significantly induced in *osvq25* mutants (Figures 5F and 5G).

OsWRKY53 increases brassinosteroid (BR) signaling, and two BR-responsive genes, *OsBU1* and *OsXTR1,* are upregulated in *OsWRKY53*-overexpression plants (Tian et al., 2017). We therefore also assessed *OsBU1* and *OsXTR1* expression in *osvq25* mutants. The expression of both genes was induced in *osvq25* mutants compared with the WT (Figures 5H and 5I). By contrast, *PR-5*, *OsBU1*, and *OsXTR1* were significantly suppressed in *ospub73* mutants (Figures S4G–S4J). Taken together, our results demonstrate that OsVQ25 suppresses the transcriptional activity of OsWRKY53, which impairs the downstream defense and growth-related BR-signaling responses.

DISCUSSION

Because crop plants growing in a region are often attacked by more than one pathogen, SNS BSR is a highly desirable trait in a crop breeding program (Li et al., 2020; Nelson et al., 2018). However, strong immune responses usually come with growth penalties (Ning et al., 2017). Therefore, SNS BSR genes that provide immunity without a growth penalty are favored by plant breeders. SNS BSR genes with potential applications in crop breeding have been identified in rice. The tetratricopeptide repeat domain RNA-binding protein Bsr-k1 negatively regulates SNS BSR (Zhou et al., 2018). *Bsr-k1* knockout in rice leads to enhanced resistance against *M. oryzae* and *Xoo* without obvious growth penalties via moderately elevating the expression of phenylalanine ammonia lyase genes (Zhou et al., 2018). In another example, *IPA1* encodes a transcription factor that reduces the number of unproductive tillers, increases the number of grains per panicle, and positively regulates SNS BSR. Upregulating *IPA1* leads to enhanced resistance against *M. oryzae* and *Xoo*, as well as improved yield (Liu et al., 2019; Wang et al., 2018). Furthermore, VQ proteins contribute to disease resistance in *Arabidopsis* (Jing and Lin, 2015), but the role of VQ protein in SNS BSR in crop plants has not been documented. In this study, we demonstrate that knockouts in the *OsVQ25* gene encoding a VQ protein increases resistance to diverse isolates of *M. oryzae* and *Xoo* in rice. Compared with the three previously reported VQ proteins (OsVQ13, OsVQ14, and OsVQ32) related to rice immunity, OsVQ25 clustered on a different branch of a phylogenetic tree (Figure S6), indicating that OsVQ25 has different functions in rice growth and disease responses. Importantly, the *osvq25* mutant presented SNS BSR with no obvious growth penalty in the major agronomic traits evaluated here. The moderately elevated activation of defense-related genes in *osvq25* may be sufficient to defend against pathogen attacks, making it a good candidate for rice breeding.

Plants use the UPS to regulate protein turnover for growth, development, and responses to abiotic and biotic stresses (Duplan and Rivas, 2014; Vierstra, 2009). In *Arabidopsis*, methyl jasmonate treatment and wounding induce the degradation of the VQ protein JAV1 via the 26S proteasome pathway in a COI1-dependent manner, but COI1 does not directly recruit JAV1 for degradation (Hu et al., 2013). The RING-type E3 ligase JUL1 interacts with and ubiquitinates JAV1, leading to its proteasomal degradation (Ali et al., 2019). *jul1* mutants have impaired resistance to *B. cinerea* and herbivorous insects, which is opposite the phenotypes of *JAV1* RNA interference lines (Ali et al., 2019; Hu et al., 2013). In this study, we established that the U-box-type E3 ligase OsPUB73 interacts with OsVQ25 and

Figure 4. Major agronomic traits measured in *osvq25* mutant lines

(A) Gross morphology of *osvq25* mutants and WT plants at the heading stage.

(B–G) Major agronomic traits measured: effective tiller number (B), thousand-grain weight (C), spike length (D), spikelet number (E), plant height (F), kernels per spike (G). For (B)–(G), values are means ± SEM ($n \geq 30$, ≥ 10, ≥ 10, ≥ 30, ≥ 30, and ≥ 10, respectively). 'ns' indicates no statistical significance at $p > 0.05$ according to Student's t test.

(H) Grain length (left) and grain width (right) of *osvq25* mutants and the WT.

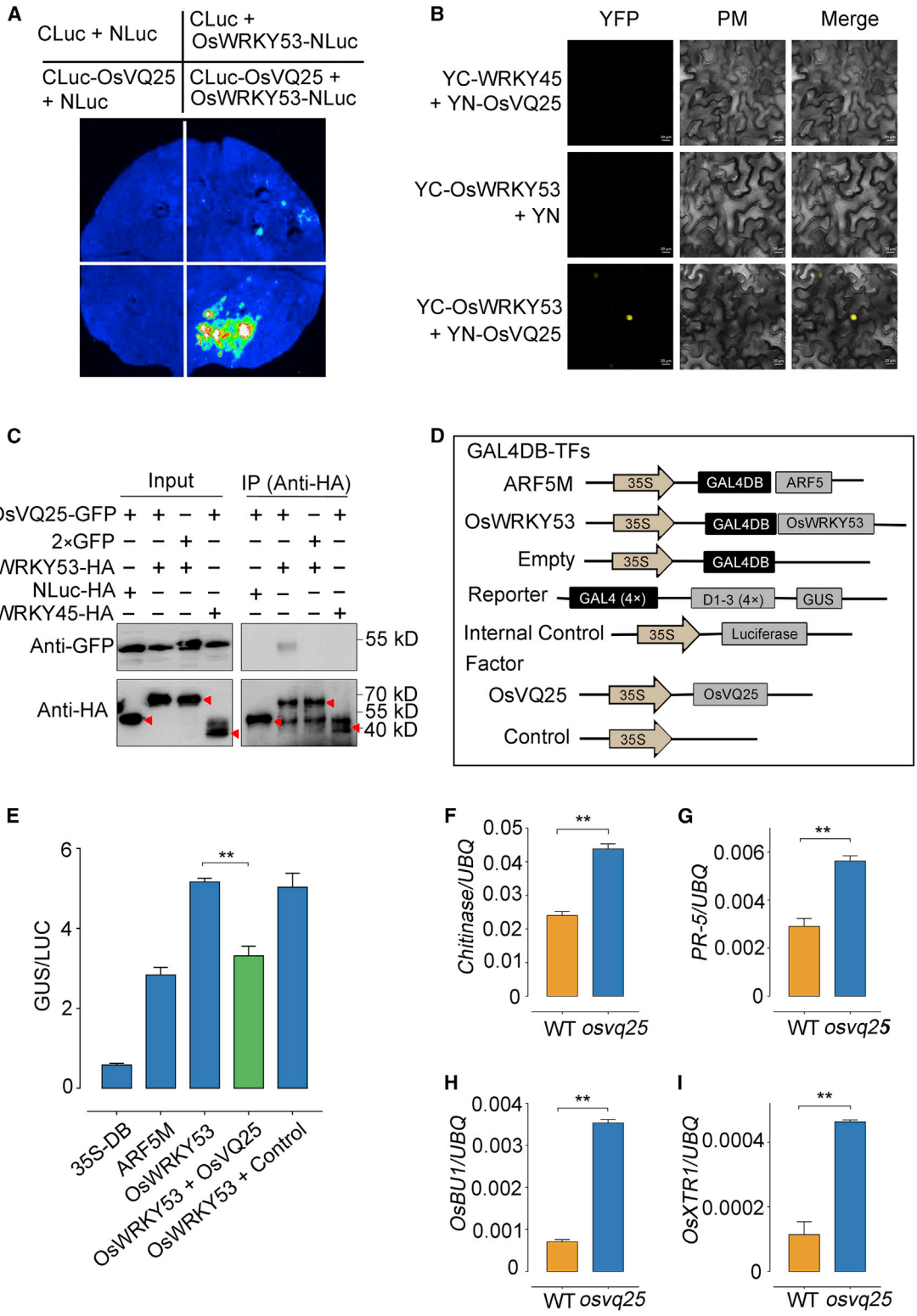

Figure 5. Interaction between OsVQ25 and OsWRKY53 and suppression of the transcriptional activity of OsWRKY53 by OsVQ25

(A) LCI assay of the interaction between OsVQ25 and OsWRKY53 in *N. benthamiana* leaves. Luminescence level was determined at 48 h after infiltration with the indicated constructs.

(legend continued on next page)

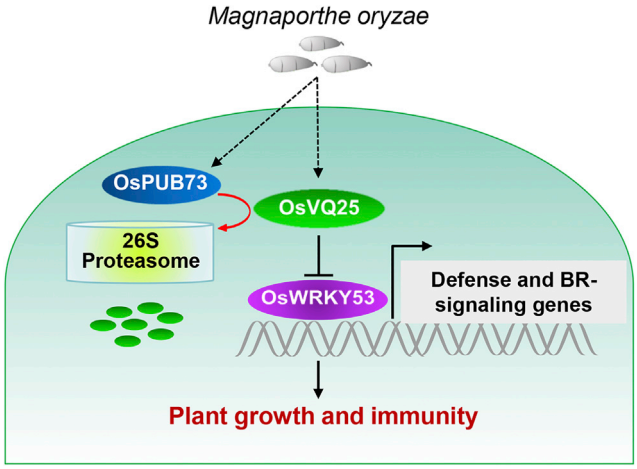

Figure 6. Working model of the role of OsVQ25 in balancing plant defense and growth

OsVQ25 negatively regulates SNS BSR. OsPUB73 promotes OsVQ25 degradation to positively regulate SNS BSR at the posttranslational level. *OsVQ25* and *OsPUB73* expression is induced by *M. oryzae* at the transcriptional level. OsVQ25 then suppresses the transcriptional activity of OsWRKY53, which consequently reduces the expression of OsWRKY53-downstream defense- and BR-signaling-related genes, to balance plant growth and defense responses.

promotes OsVQ25 degradation via the UPS in rice. The *ospub73* mutants had reduced resistance to *M. oryzae* and *Xoo*, which was opposite the *osvq25* phenotype. Our results suggest that OsVQ25 is a substrate of OsPUB73 in rice, and it comprises an example of E3 ligase-VQ protein module in crop plants. While the E3-type proteins SPL11, EBR1, and OsCUL3a negatively regulate SNS BSR (Liu et al., 2017; You et al., 2016; Zeng et al., 2004), we demonstrated here that *OsPUB73* positively regulates SNS BSR. Furthermore, OsPUB73 is required for anther development, and *ospub73* knockouts in rice display low pollen fertility (Chen et al., 2019), suggesting that OsPUB73 positively regulates rice development. These results indicate that OsPUB73 modulates OsVQ25 at the posttranslational level to regulate the balance between immunity and growth.

VQ proteins interact with WRKY TFs and affect downstream processes in *Arabidopsis* (Jing and Lin, 2015). For instance, JAV1 interacts with WRKY28 and WRKY51, functioning as a positive regulator of WRKY28 and as a negative regulator of WRKY51 (Hu et al., 2013). JAV1 and JAZ8 interact with WRKY51 to form a so-called JJW (JAV1-JAZ8-WRKY51) complex that represses the expression of JA biosynthesis genes. JAV1 phosphorylation, which is triggered by injury, causes the JJW complex to disintegrate, thus alleviating the prior repression and leading to the activation of JA biosynthesis (Yan et al., 2018). In rice, expression pattern analysis in different tissues and developmental stages indicated that 12 out of 40 VQ genes are co-expressed with 20 *WRKY* genes (Li et al., 2014), but no studies have reported that VQs and WRKYs interact with each other. Here, we showed that OsVQ25 interacts with OsWRKY53 and suppresses OsWRKY53 transcriptional activity. OsWRKY53 is a typical transcription factor (Chujo et al., 2007). *OsWRKY53* expression is induced by treatment with the oligosaccharide elicitor chitin and by *M. oryzae* infection. *OsWRKY53* overexpression increases resistance to *M. oryzae* (Chujo et al., 2007, 2014). We determined that loss of *OsWRKY53* function decreases the resistance to *M. oryzae*. Furthermore, the expression of defense-related genes *PR-5* and *Chitinase*, which are positively regulated by OsWRKY53, increased in *osvq25* mutants. In addition, the BR-responsive genes *OsBU1* and *OsXTR1*, also positively regulated by OsWRKY53 (Tian et al., 2017), were also upregulated in *osvq25*. *oswrky53* mutant plants were slightly dwarf and had more erect leaves, but *OsWRKY53* overexpression results in enlarged leaf angles and significantly decreased plant height, which did not occur in *osvq25* mutant lines (Xie et al., 2021). It is possible that the moderately increased expression levels of BR-responsive genes in *osvq25* mutants maintain, but are not enough to alter, the key agronomic traits of *osvq25* mutants in the field. Thus, our results demonstrate that OsVQ25 modulates the transcriptional activity of OsWRKY53 to balance immunity and growth in rice. Remarkably, OsWRKY53 negatively regulates rice resistance to *Xoo* (Xie et al., 2021). *OsWRKY53* overexpression reduced resistance to *Xoo*, while its knockout enhanced the strength of resistance. However, defense-related genes, including *Chitinase*, are induced in *OsWRKY53*-overexpression plants (Xie et al., 2021), which is consistent with the report that OsWRKY53 positively regulates *M. oryzae* resistance (Chujo et al., 2007, 2014), indicating that the resistance mechanisms mediated by OsWRKY53 differ for *M. oryzae* and *Xoo*. Therefore, there might be another pathway regulated by OsVQ25 that positively regulates resistance to *Xoo*.

We propose the following regulatory model of how OsPUB73, OsVQ25, and OsWRKY53 interact to balance immunity and growth in rice (Figure 6). OsVQ25 negatively regulates SNS BSR to *M. oryzae*. The U-box-type E3 ligase OsPUB73 interacts with and promotes OsVQ25 degradation via the UPS to positively regulate SNS BSR. By reducing the transcriptional activity of

(B) BiFC assay to test the interaction between OsVQ25 and OsWRKY53 in *N. benthamiana* leaves. YFP fluorescence was acquired from *N. benthamiana* leaf cells on a confocal microscope at 48 h after infiltration of the indicated constructs. Scale bar, 20 μm.

(C) Co-IP assay to test the interaction between OsVQ25 and OsWRKY53 in rice protoplasts. Total protein was extracted from rice protoplasts transfected with the indicated constructs, followed by immunoprecipitation with anti-HA antibody. Red arrowheads indicate the expected proteins. There were three biological replicates with similar results.

(D) Constructs used in the transcriptional activity assay in (E).

(E) OsVQ25 suppresses the transcriptional activity of WRKY53. We used ARF5M, a transcription activator, as a control. Asterisks indicate a significant difference between OsWRKY53 and the OsWRKY53 + OsVQ25 combination. Values are means ± SEM (n = 3 biological replicates).

(F and G) Relative transcript levels of the OsWRKY53-downstream defense-related genes *Chitinase* (F) and *PR-5* (G) in *osvq25* mutants and WT plants, as determined by qRT-PCR. We used rice *UBIQUITIN* (*UBQ*) as the reference gene to normalize gene expression. Values are means ± SEM (n = 3 biological replicates).

(H and I) Relative transcript levels of the OsWRKY53-downstream BR-signaling genes *OsBU1* (H) and *OsXTR1* (I) in *osvq25* mutants and WT plants, as determined by qRT-PCR. Values are means ± SEM (n = 3 biological replicates). Asterisks in (E)–(I) indicate statistical significance (**$p \leq 0.01$, Student's t test).

OsWRKY53, OsVQ25 suppresses downstream defense signaling and BR signaling, balancing plant defense responses and growth in rice. Our results highlight the hierarchical regulatory mechanism of an OsPUB73-OsVQ25-OsWRKY53 module that balances BSR and plant growth in rice, proposing a new insight for breeding SNS BSR rice varieties as well as other agriculturally important crop plants for improved food security and sustainable agriculture.

Limitations of the study

Although we demonstrated that the VQ protein OsVQ25 is a substrate of the E3 ligase OsPUB73, we cannot exclude the possibility that there are other substrates of OsPUB73, or that other E3 ligases or pathways promote OsVQ25 degradation. OsVQ25 negatively regulates resistance to *M. oryzae* and *Xoo* and hinders the transcriptional activity of OsWRKY53 to suppress *M. oryzae* resistance in rice, but the molecular mechanism by which OsVQ25 suppresses OsWRKY53 transcriptional activity remains unclear. In addition, our model only presents how OsVQ25 regulates *M. oryzae* resistance in rice. It is likely that there are other target proteins or mechanisms by which OsVQ25 modulates *Xoo* resistance. Future study is needed to investigate the OsVQ25 downstream signaling cascade to better understand the molecular mechanism of OsVQ25-mediated SNS BSR.

STAR★METHODS

Detailed methods are provided in the online version of this paper and include the following:

- KEY RESOURCES TABLE
- RESOURCE AVAILABILITY
  - Lead contact
  - Materials availability
  - Data and code availability
- EXPERIMENTAL MODEL AND SUBJECT DETAILS
  - *Oryza sativa*
  - *Nicotiana benthamiana*
  - *Arabidopsis thaliana*
- METHOD DETAILS
  - Expression pattern analysis
  - *M. oryzae* inoculation and disease symptom evaluation
  - *Xanthomonas oryzae* pv. *oryzae* (*Xoo*) inoculation and disease symptom evaluation
  - Luciferase complementation imaging (LCI) assay in *N. benthamiana*
  - *In vivo* co-immunoprecipitation assay
  - Bimolecular fluorescence complementation assay in *N. benthamiana*
  - Protein degradation assay in rice protoplasts
  - Transcriptional activity assay in arabidopsis protoplasts
  - Electrophoretic mobility shift assay
  - Dual-luciferase assay in rice protoplasts
  - RNA extraction and quantitative reverse transcriptase PCR
  - Accession numbers
- QUANTIFICATION AND STATISTICAL ANALYSIS

SUPPLEMENTAL INFORMATION

Supplemental information can be found online at https://doi.org/10.1016/j.celrep.2022.111235.

ACKNOWLEDGMENTS

This work was supported by grants from the National Natural Science Foundation of China (32161143009, 31822041, and 31972225) to Y.N., the Major Research Plan of the National Natural Science Foundation of China (3218810004) to L.X., and the National Natural Science Foundation of China (U20A2021) to R.W.

AUTHOR CONTRIBUTIONS

Y.N. and L.X. conceived the project. Z.H., J.T., H.F., L.F., X.X., F.H., S.L., W.X., Q.D., X.Y., D.W., Q.C., S.Z., and R.W. carried out the experiments. Z.H, J.T, H.F. S.L., and M.Y. performed the transgenic plant generation and analysis. Z.H., J.T., and H.F. wrote the paper. Y.N., L.X., and G.L.W. analyzed the data and revised the manuscript.

DECLARATION OF INTERESTS

The authors declare no competing interests.

Received: December 1, 2021
Revised: June 17, 2022
Accepted: July 27, 2022
Published: August 16, 2022

REFERENCES

Ali, M.R.M., Uemura, T., Ramadan, A., Adachi, K., Nemoto, K., Nozawa, A., Hoshino, R., Abe, H., Sawasaki, T., and Arimura, G.I. (2019). The ring-type E3 ubiquitin ligase JUL1 targets the VQ-motif protein JAV1 to coordinate jasmonate signaling. Plant Physiol. *179*, 1273–1284.

Andreasson, E., Jenkins, T., Brodersen, P., Thorgrimsen, S., Petersen, N.H.T., Zhu, S., Qiu, J.L., Micheelsen, P., Rocher, A., Petersen, M., et al. (2005). The MAP kinase substrate MKS1 is a regulator of plant defense responses. EMBO J. *24*, 2579–2589.

Chen, L., Deng, R., Liu, G., Jin, J., Wu, J., and Liu, X. (2019). Cytological and transcriptome analyses reveal OsPUB73 defect affects the gene expression associated with tapetum or pollen exine abnormality in rice. BMC Plant Biol. *19*, 546.

Chi, Y., Yang, Y., Zhou, Y., Zhou, J., Fan, B., Yu, J.Q., and Chen, Z. (2013). Protein-protein interactions in the regulation of WRKY transcription factors. Mol. Plant *6*, 287–300.

Chujo, T., Miyamoto, K., Ogawa, S., Masuda, Y., Shimizu, T., Kishi-Kaboshi, M., Takahashi, A., Nishizawa, Y., Minami, E., Nojiri, H., et al. (2014). Overexpression of phosphomimic mutated OsWRKY53 leads to enhanced blast resistance in rice. PLoS One *9*, e98737.

Chujo, T., Takai, R., Akimoto-Tomiyama, C., Ando, S., Minami, E., Nagamura, Y., Kaku, H., Shibuya, N., Yasuda, M., Nakashita, H., et al. (2007). Involvement of the elicitor-induced gene OsWRKY53 in the expression of defense-related genes in rice. Biochim. Biophys. Acta *1769*, 497–505.

Clarke, J.D. (2009). Cetyltrimethyl ammonium bromide (CTAB) DNA miniprep for plant DNA isolation. Cold Spring Harb. Protoc. *2009*. pdb.prot5177.

Duplan, V., and Rivas, S. (2014). E3 ubiquitin-ligases and their target proteins during the regulation of plant innate immunity. Front. Plant Sci. *5*, 42.

Fan, J., Bai, P., Ning, Y., Wang, J., Shi, X., Xiong, Y., Zhang, K., He, F., Zhang, C., Wang, R., et al. (2018). The monocot-specific receptor-like kinase SDS2 controls cell death and immunity in rice. Cell Host Microbe *23*, 498–510.e5.

Fang, H., Shen, S., Wang, D., Zhang, F., Zhang, C., Wang, Z., Zhou, Q., Wang, R., Tao, H., He, F., et al. (2021). A monocot-specific hydroxycinnamoylputrescine gene cluster contributes to immunity and cell death in rice. Sci. Bull. *66*, 2381–2393.

Fiil, B.K., and Petersen, M. (2011). Constitutive expression of MKS1 confers susceptibility to Botrytis cinerea infection independent of PAD3 expression. Plant Signal. Behav. *6*, 1425–1427.

Hu, P., Zhou, W., Cheng, Z., Fan, M., Wang, L., and Xie, D. (2013). JAV1 controls jasmonate-regulated plant defense. Mol. Cell *50*, 504–515.

Jiang, S.Y., Sevugan, M., and Ramachandran, S. (2018). Valine-glutamine (VQ) motif coding genes are ancient and non-plant-specific with comprehensive expression regulation by various biotic and abiotic stresses. BMC Genom. *19*, 342.

Jing, Y., and Lin, R. (2015). The VQ motif-containing protein family of plant-specific transcriptional regulators. Plant Physiol. *169*, 371–378.

Ke, Y., Deng, H., and Wang, S. (2017). Advances in understanding broad-spectrum resistance to pathogens in rice. Plant J. *90*, 738–748.

Kim, D.Y., Kwon, S.I., Choi, C., Lee, H., Ahn, I., Park, S.R., Bae, S.C., Lee, S.C., and Hwang, D.J. (2013). Expression analysis of rice VQ genes in response to biotic and abiotic stresses. Gene *529*, 208–214.

Kou, Y., and Wang, S. (2010). Broad-spectrum and durability: understanding of quantitative disease resistance. Curr. Opin. Plant. Biol. *13*, 181–185.

Lai, Z., Li, Y., Wang, F., Cheng, Y., Fan, B., Yu, J.Q., and Chen, Z. (2011). Arabidopsis sigma factor binding proteins are activators of the WRKY33 transcription factor in plant defense. Plant Cell *23*, 3824–3841.

Li, N., Li, X., Xiao, J., and Wang, S. (2014). Comprehensive analysis of VQ motif-containing gene expression in rice defense responses to three pathogens. Plant Cell Rep. *33*, 1493–1505.

Li, N., Yang, Z., Li, J., Xie, W., Qin, X., Kang, Y., Zhang, Q., Li, X., Xiao, J., Ma, H., and Wang, S. (2021). Two VQ proteins are substrates of the OsMPKK6-OsMPK4 cascade in rice defense against bacterial blight. Rice *14*, 39.

Li, W., Deng, Y., Ning, Y., He, Z., and Wang, G.L. (2020). Exploiting broad-spectrum disease resistance in crops: from molecular dissection to breeding. Annu. Rev. Plant Biol. *71*, 575–603.

Liu, J., Park, C.H., He, F., Nagano, M., Wang, M., Bellizzi, M., Zhang, K., Zeng, X., Liu, W., Ning, Y., et al. (2015). The RhoGAP SPIN6 associates with SPL11 and OsRac1 and negatively regulates programmed cell death and innate immunity in rice. PLoS Pathog. *11*, e1004629.

Liu, M., Shi, Z., Zhang, X., Wang, M., Zhang, L., Zheng, K., Liu, J., Hu, X., Di, C., Qian, Q., et al. (2019). Inducible overexpression of Ideal Plant Architecture1 improves both yield and disease resistance in rice. Nat. Plants *5*, 389–400.

Liu, Q., Ning, Y., Zhang, Y., Yu, N., Zhao, C., Zhan, X., Wu, W., Chen, D., Wei, X., Wang, G.L., et al. (2017). OsCUL3a negatively regulates cell death and immunity by degrading OsNPR1 in rice. Plant Cell *29*, 345–359.

Ma, X., Zhang, Q., Zhu, Q., Liu, W., Chen, Y., Qiu, R., Wang, B., Yang, Z., Li, H., Lin, Y., et al. (2015). A robust CRISPR/Cas9 system for convenient, high-efficiency multiplex genome editing in monocot and dicot plants. Mol. Plant *8*, 1274–1284.

Nelson, R., Wiesner-Hanks, T., Wisser, R., and Balint-Kurti, P. (2018). Navigating complexity to breed disease-resistant crops. Nat. Rev. Genet. *19*, 21–33.

Ning, Y., Liu, W., and Wang, G.L. (2017). Balancing immunity and yield in crop plants. Trends. Plant. Sci. *22*, 1069–1079.

Ning, Y., Wang, R., Shi, X., Zhou, X., and Wang, G.L. (2016). A layered defense strategy mediated by rice E3 ubiquitin ligases against diverse pathogens. Mol. Plant *9*, 1096–1098.

Petersen, K., Qiu, J.L., Lütje, J., Fiil, B.K., Hansen, S., Mundy, J., and Petersen, M. (2010). Arabidopsis MKS1 is involved in basal immunity and requires an intact N-terminal domain for proper function. PLoS One *5*, e14364.

Shi, X., Long, Y., He, F., Zhang, C., Wang, R., Zhang, T., Wu, W., Hao, Z., Wang, Y., Wang, G.L., and Ning, Y. (2018). The fungal pathogen Magnaporthe oryzae suppresses innate immunity by modulating a host potassium channel. PLoS Pathog. *14*, e1006878.

Sadanandom, A., Bailey, M., Ewan, R., Lee, J., and Nelis, S. (2012). The ubiquitin-proteasome system: central modifier of plant signalling. New. Phytol. *196*, 13–28.

Tian, X., Li, X., Zhou, W., Ren, Y., Wang, Z., Liu, Z., Tang, J., Tong, H., Fang, J., and Bu, Q. (2017). Transcription factor OsWRKY53 positively regulates brassinosteroid signaling and plant architecture. Plant. Physiol. *175*, 1337–1349.

Uji, Y., Kashihara, K., Kiyama, H., Mochizuki, S., Akimitsu, K., and Gomi, K. (2019). Jasmonic acid-induced VQ-motif-containing protein OsVQ13 influences the OsWRKY45 signaling pathway and grain size by associating with OsMPK6 in rice. Int. J. Mol. Sci. *20*, 2917.

Vierstra, R.D. (2009). The ubiquitin-26S proteasome system at the nexus of plant biology. Nat. Rev. Mol. Cell. Biol. *10*, 385–397.

Wang, J., Wang, R., Fang, H., Zhang, C., Zhang, F., Hao, Z., You, X., Shi, X., Park, C.H., Hua, K., et al. (2021). Two VOZ transcription factors link an E3 ligase and an NLR immune receptor to modulate immunity in rice. Mol. Plant *14*, 253–266.

Wang, J., Zhou, L., Shi, H., Chern, M., Yu, H., Yi, H., He, M., Yin, J., Zhu, X., Li, Y., et al. (2018). A single transcription factor promotes both yield and immunity in rice. Science *361*, 1026–1028.

Wang, R., Ning, Y., Shi, X., He, F., Zhang, C., Fan, J., Jiang, N., Zhang, Y., Zhang, T., Hu, Y., et al. (2016). Immunity to rice blast disease by suppression of effector-triggered necrosis. Curr. Biol. *26*, 2399–2411.

Xie, W., Ke, Y., Cao, J., Wang, S., and Yuan, M. (2021). Knock out of transcription factor WRKY53 thickens sclerenchyma cell walls, confers bacterial blight resistance. Plant Physiol. *187*, 1746–1761.

Xie, Y.D., Li, W., Guo, D., Dong, J., Zhang, Q., Fu, Y., Ren, D., Peng, M., and Xia, Y. (2010). The Arabidopsis gene SIGMA FACTOR-BINDING PROTEIN 1 plays a role in the salicylate- and jasmonate-mediated defence responses. Plant. Cell. Environ. *33*, 828–839.

Yan, C., Fan, M., Yang, M., Zhao, J., Zhang, W., Su, Y., Xiao, L., Deng, H., and Xie, D. (2018). Injury activates Ca(2+)/calmodulin-dependent phosphorylation of JAV1-JAZ8-WRKY51 complex for jasmonate biosynthesis. Mol. Cell *70*, 136–149.e7.

Yoo, S.D., Cho, Y.H., and Sheen, J. (2007). Arabidopsis mesophyll protoplasts: a versatile cell system for transient gene expression analysis. Nat. Protoc. *2*, 1565–1572.

You, Q., Zhai, K., Yang, D., Yang, W., Wu, J., Liu, J., Pan, W., Wang, J., Zhu, X., Jian, Y., et al. (2016). An E3 ubiquitin ligase-BAG protein module controls plant innate immunity and broad-spectrum disease resistance. Cell Host Microbe *20*, 758–769.

You, X., Zhu, S., Zhang, W., Zhang, J., Wang, C., Jing, R., Chen, W., Wu, H., Cai, Y., Feng, Z., et al. (2019). OsPEX5 regulates rice spikelet development through modulating jasmonic acid biosynthesis. New Phytol. *224*, 712–724.

Zeng, L.R., Park, C.H., Venu, R.C., Gough, J., and Wang, G.L. (2008). Classification, expression pattern, and E3 ligase activity assay of rice U-box-containing proteins. Mol. Plant *1*, 800–815.

Zeng, L.R., Qu, S., Bordeos, A., Yang, C., Baraoidan, M., Yan, H., Xie, Q., Nahm, B.H., Leung, H., and Wang, G.L. (2004). Spotted leaf11, a negative regulator of plant cell death and defense, encodes a U-box/armadillo repeat protein endowed with E3 ubiquitin ligase activity. Plant Cell *16*, 2795–2808.

Zeng, L.R., Vega-Sánchez, M.E., Zhu, T., and Wang, G.L. (2006). Ubiquitination-mediated protein degradation and modification: an emerging theme in plant-microbe interactions. Cell Res. *16*, 413–426.

Zhang, C., Fang, H., Shi, X., He, F., Wang, R., Fan, J., Bai, P., Wang, J., Park, C.H., Bellizzi, M., et al. (2020). A fungal effector and a rice NLR protein have antagonistic effects on a Bowman-Birk trypsin inhibitor. Plant Biotechnol. J. *18*, 2354–2363.

Zhou, X., Liao, H., Chern, M., Yin, J., Chen, Y., Wang, J., Zhu, X., Chen, Z., Yuan, C., Zhao, W., et al. (2018). Loss of function of a rice TPR-domain RNA-binding protein confers broad-spectrum disease resistance. Proc. Natl. Acad. Sci. USA *115*, 3174–3179.

STAR★METHODS

KEY RESOURCES TABLE

REAGENT or RESOURCE	SOURCE	IDENTIFIER
Antibodies		
Mouse monoclonal anti-HA	Roche	Cat# 11867431001; RRID: AB_390919
Mouse monoclonal anti-GFP	Roche	Cat# 11814460001; RRID: AB_390913
Mouse monoclonal anti-Actin	ABclonal	Cat# AC009; RRID: AB_2771701
Bacterial and virus strains		
Escherichia coli strain DH5a	Tsingke	Cat# TSC-C01
Escherichia coli strain BL21(DE3)	Tsingke	Cat# TSC-E01
Agrobacterium tumefaciens strain EHA105	This paper	N/A
Magnaporthe oryzae strain RO1-1	This paper	N/A
Magnaporthe oryzae strain RB22	This paper	N/A
Chemicals, peptides, and recombinant proteins		
MG-132	Selleck Chemicals LLC	Cat# S2619
Protease Inhibitor Cocktail, EDTA free	Roche	Cat# 04693159001
TRIzolTM	Invitrogen	Cat# 15596018
ChamQ SYBR qPCR Master Mix	Vazyme	Cat# Q311-03
HiScript II Q RT SuperMix for qPCR (+gDNA wiper)	Vazyme	Cat# R223-01
Cycloheximide	Cell Signaling	Cat# 2112
Critical commercial assays		
Dual-Luciferase Reporter Assay System	Vazyme	Cat# DD1205-01
T4 Polynucleotide Kinase	Thermo ScientificTM	Cat# EK003
Experimental models: Organisms/strains		
Oryza Sativa: Nipponbare wild type	This paper	N/A
Oryza Sativa: Zhonghua 11 wild type	Xie et al. (2021)	N/A
Oryza Sativa: *osvq25*	This paper	N/A
Oryza Sativa: *ospub73*	This paper	N/A
Oryza Sativa: *oswrky53*	Xie et al. (2021)	N/A
Nicotiana benthamiana	This paper	N/A
Arabidopsis	This paper	N/A
Oligonucleotides		
See Table S1	This paper	N/A
Recombinant DNA		
35S:OsVQ25-CLuc	This Paper	N/A
35S:OsPUB73-NLuc	This Paper	N/A
35S:OsWRKY53-NLuc	This Paper	N/A
35S:WRKY45-NLuc	This Paper	N/A
35S:GFP-GFP	This Paper	N/A
Ubi:OsVQ25-GFP	This Paper	N/A
Ubi:OsPUB73-HA	This Paper	N/A
Ubi:OsPUB73-C-HA	This Paper	N/A
Ubi:OsWRKY53-HA	This Paper	N/A
Ubi:NLuc-HA	This Paper	N/A
35S:OsVQ25-YFP^N	This Paper	N/A
35S:YFP^C-OsPUB73	This Paper	N/A
35S:YFP^C-OsWRKY53	This Paper	N/A

(*Continued on next page*)

Continued		
REAGENT or RESOURCE	SOURCE	IDENTIFIER
35S:YFP^{C}-WRKY45	This Paper	N/A
35S:OsVQ25	This Paper	N/A
35S:GAL4DB-OsWRKY53	This Paper	N/A
35S:GAL4DB-ARF5M	Wang et al. (2021)	N/A
35S:OsWRKY53	Xie et al. (2021)	N/A
ProOsMYB63:LUC	Xie et al. (2021)	N/A

RESOURCE AVAILABILITY

Lead contact

Further information and requests for resources and reagents should be directed to and will be fulfilled by the lead contact, Yuese Ning (ningyuese@caas.cn).

Materials availability

All materials generated in this study are available from the lead contact. This study did not generate new unique reagents.

Data and code availability

The data reported in this paper will be shared by the lead contact upon request.
This paper does not report original code.
Any additional information required to reanalyze the data reported in this paper is available from the lead contact upon request.

EXPERIMENTAL MODEL AND SUBJECT DETAILS

Oryza sativa

The rice (*Oryza sativa*) cultivars Nipponbare (NPB) and Zhonghua11 (ZH11) were used for disease evaluation in this study. Rice seeds were surface-sterilized by immersion in 75% (v/v) ethanol for 5 min, followed by immersion in 40% (v/v) sodium hypochlorite for 25 min. After washing 5 times with sterile water, the seeds were germinated on 1/2 Murashige Skoog (MS) medium for 1 week. The seedlings were then maintained in an incubator with a 12-h light/12-h dark photoperiod, a 28/26°C light/dark temperature regime, and 65% relative humidity. After 7 days in the incubator, the seedlings were transferred to soil and maintained in a growth chamber at 26°C with a 12-h light/12-h dark photoperiod and 70% relative humidity.

The CRISPR/Cas9 system and rice variety NPB were used to generate the *osvq25* and *ospub73* knockout mutants. The single guide RNA (sgRNA) sequence was designed to specifically target the genomic loci of *OsVQ25* and *OsPUB73*. The sgRNA expression cassette was then inserted into the pYLCRISPR/Cas9-MTmono binary vector (Ma et al., 2015). The resulting constructs were introduced into *Agrobacterium* (*Agrobacterium tumefaciens*) strain EHA105 for rice transformation. *oswrky53* mutant plants and ZH11 were described previously (Xie et al., 2021). All primer sequences used for the constructs are listed in Table S1.

Nicotiana benthamiana

N. benthamiana plants were cultivated in soil under a 12-h light/12-h dark photoperiod at 25°C. Five-week-old *N. benthamiana* leaves were used in luciferase complementation imaging and bimolecular fluorescence complementation assays.

Arabidopsis thaliana

Arabidopsis (*Arabidopsis thaliana*) accession Columbia-0 (Col-0) were cultivated in soil at 25°C with a 16/8 h light/dark cycle. Five-week-old Arabidopsis leaves were used for the transcriptional activity assay.

METHOD DETAILS

Expression pattern analysis

Rice leaves were collected at different time points after spray inoculation with *Magnaporthe oryzae* isolates. Water with 0.05% (v/v) Tween 20 was used as a mock inoculation control (Mock) (Fang et al., 2021). Total RNA was isolated with Trizol reagent (Invitrogen) according to the manufacturer's instructions. First-strand cDNA was synthesized with reverse transcriptase (Promega) after digestion of total RNA with DNase I (TransGen). qRT-PCR was performed with 2×SYBR Green Mix (GeneStar) on an ABI Prism 7500 PCR instrument. Gene expression levels were calculated with the data from three technical replicates. The primer sequences used for the qRT-PCR assay are listed in Table S1.

M. oryzae inoculation and disease symptom evaluation

M. oryzae isolates were cultivated on oatmeal agar plates under weak light for 14 days to generate spores. Six-week-old rice plants were used for punch inoculation (Fang et al., 2021) with a suspension of *M. oryzae* spores (about 5×10^5 spores/mL). After a mouse ear clip was used to lightly punch rice leaves, the punched sites were treated with one drop (10 μL) of the spore suspension. The spores were held in place by sealing both sides of the treated sites with scotch tape. Two weeks after inoculation, the inoculated leaves were photographed. A 4-cm-long segment of rice leaf with lesion was then cut and subjected to DNA extraction with the cetyltrimethyl ammonium bromide (CTAB) protocol (Clarke, 2009). Relative fungal biomass was measured as previously described with DNA-based quantitative PCR (qPCR) using the threshold cycle value (Ct) of *M. oryzae MoPot2* and rice genomic *UBIQUITIN* (*OsUbq*) according to the formula $2^{[CT(OsUbq)-CT(MoPot2)]}$ (Shi et al., 2018). qPCR was performed with 2×SYBR Green Mix (GeneStar) on an ABI Prism 7500 PCR instrument.

Xanthomonas oryzae pv. *oryzae* (*Xoo*) inoculation and disease symptom evaluation

Xoo isolates were cultured on potato dextrose liquid medium (30°C, 200 rpm) until the optical density (OD_{600}) of the culture was 1.0 (Liu et al., 2017); the resulting suspension was used to inoculate rice leaves. Leaves of 6-week-old rice plants were cut with a scissors that had been dipped into the bacterial suspension (Liu et al., 2017). Two weeks after inoculation, the inoculated leaves were photographed and lesion lengths were measured.

Luciferase complementation imaging (LCI) assay in *N. benthamiana*

The LCI assay was performed in *N. benthamiana* as previously described (Zhang et al., 2020). The coding sequences of *OsPUB73* and *OsWRKY53* were cloned into the pCAMBIA-NLuc vector (*OsPUB73-NLuc*, *OsWRKY53-NLuc*), and the coding sequence of *OsVQ25* was cloned into the pCAMBIA-CLuc vector (*CLuc-OsVQ25*). *Agrobacterium* cultures (strain EHA105) individually containing the respective constructs, were adjusted to an OD_{600} of 0.5 with MES buffer (10 mM $MgCl_2$, 10 mM MES and 0.2mM acetosyringone, pH 5.6) and used for co-infiltration of *N. benthamiana* leaves. At 48 h after co-infiltration, infiltrated leaves were incubated with 150 ng/mL D-luciferin potassium salt and photographed with NightSHADE LB 985 *in vivo* plant imager to qualitatively measure LUC activity. Leaf discs were then taken and incubated with 150 ng/mL D-luciferin potassium salt in a 96-well plate, and the relative LUC activity was quantified with a GLOMAX 96 microplate luminometer (Promega). All primer sequences used for the constructs are listed in Table S1.

In vivo co-immunoprecipitation assay

Co-immunoprecipitation (Co-IP) assays were performed as previously described (Wang et al., 2016). The desired constructs were co-transfected into rice protoplasts, 20 μM MG132 was added to the treated rice protoplasts at 12 h after co-transfection, and 12 h later, total protein was extracted in native buffer (50 mM Tris-MES, pH 8.0, 0.5 M sucrose, 1 mM $MgCl_2$, 10 mM EDTA, 5 mM DTT, 50 μM MG132, and protease inhibitor cocktail). The proteins were then incubated with anti-HA antibody with gentle shaking for 6 h at 4°C before 25 μL of pre-rinsed Protein G beads (Millipore) was added to the protein-antibody samples, after which the preparation was incubated for another 3 h. The beads were then washed 3–5 times with 1×phosphate buffered saline with 1% Tween-20 (PBST) buffer before 1×SDS loading buffer was added to each sample, which was boiled for 8 min. About 10 μL of each sample was separated by SDS-PAGE for immunoblot analysis. All primer sequences used for the constructs are listed in Table S1.

Bimolecular fluorescence complementation assay in *N. benthamiana*

For the bimolecular fluorescence complementation (BiFC) assays, full-length coding sequences of *OsVQ25*, *OsPUB73*, *OsWRKY53*, and *WRKY45* were individually cloned into the p2YN (nYFP) or p2YC (cYFP) vectors to produce the fusion to the N- or C-terminal half of YFP (You et al., 2019), including p2YN-OsVQ25, p2YC-OsPUB73, p2YC-OsWRKY53, and p2YC-WRKY45. The resulting plasmids were separately transformed into *Agrobacterium* (strain EHA105) and then transiently infiltrated in *N. benthamiana* leaves. Fluorescent signals were observed using a laser scanning confocal microscope (Zeiss LSM880) between 48 and 72 h after infiltration. All primer sequences used for the constructs are listed in Table S1.

Protein degradation assay in rice protoplasts

Protein degradation assays in rice protoplasts were performed as previously described (Wang et al., 2021). Briefly, 12 h after the desired constructs were co-transfected into rice protoplasts, 20 μM MG132 was added to the transfected protoplasts, and 12 h later, the rice protoplasts were harvested for protein extraction. Total protein was extracted with denaturation buffer (50 mM Tris-HCl, pH 7.5, 150 mM NaCl, 0.5% [v/v] NP40, 4 M urea, and 1 mM PMSF). Protein abundance was detected by immunoblotting and normalized to rice ACTIN levels in each sample. In addition, total RNA was isolated, and the relative transcript levels of each gene were determined by RT-PCR. All primer sequences used for the constructs are listed in Table S1.

Transcriptional activity assay in arabidopsis protoplasts

The transcriptional activity assay in Arabidopsis protoplasts was performed as previously described (Wang et al., 2021). The *GUS* reporter gene was cloned downstream of four GAL4 DNA-binding sites and four tandem copies of the constitutive D1-3 element (GAL4(4X)–D1-3(4X)). The *OsWRKY53* full-length coding sequence was cloned in-frame with the sequence of *GAL4-DB* under the

control of the cauliflower mosaic virus (CaMV) 35S promoter to obtain the *GAL4DB-OsWRKY53* construct. The 35S promoter was also used to drive the firefly *LUC* gene as the internal control. The *OsVQ25* coding sequence was cloned into the pGreenII 62-SK vector and placed under the control of the 35S promoter as an effector. All primer sequences used for the constructs are listed in Table S1.

Arabidopsis protoplasts were isolated from the leaves of approximately 5-week-old WT (Columbia-0) plants, and polyethylene glycol (PEG)-mediated transformation was used for transfection as previously described (Yoo et al., 2007). LUC and GUS activities were measured with a GLOMAX 96 microplate luminometer (Promega) (Promega) and a FlexStation 3 (Molecular Devices), respectively. The GUS/LUC ratios were used to evaluate the transcriptional activity of OsWRKY53.

Electrophoretic mobility shift assay

Recombinant His-OsWRKY53 protein was prepared as described previously (Xie et al., 2021). The plasmids harboring the *OsVQ25* coding sequences were introduced into *Escherichia coli* BL21(DE3) cells, and then 0.2 mM isopropylthio-b-galactoside (IPTG) was added to induce protein production overnight at 16°C, and the proteins were purified using Amylose Resin (BioLabs, #E8021V). The electrophoretic mobility shift assay (EMSA) and 5′-FAM-modified oligonucleotide probes containing W-box elements from *OsMYB63* promoter regions were described previously (Xie et al., 2021).

Dual-luciferase assay in rice protoplasts

The dual-luciferase assay in rice protoplasts and reporter constructs used in this assay were described previously (Xie et al., 2021). The *OsVQ25* effector construct was co-transfected with effector and reporter constructs into rice protoplasts to test the effect of OsVQ25 on *OsWRKY53* transcription. The protoplasts were collected 24 h after transfection with the indicated combinations. The LUC and REN activities were measured according to the manufacturer's instructions (Promega, USA). The relative reporter gene expression level was calculated as the ratio between LUC and REN activity.

RNA extraction and quantitative reverse transcriptase PCR

Total RNA isolation and quantitative reverse transcriptase PCR (qRT-PCR) were performed as previously described (Fang et al., 2021). Total RNA was extracted from rice tissues using a plant RNA extraction kit (Sangon Biotech, Shanghai, China). For RT-qPCR, 2 μg of total RNA was reverse transcribed into first-strand cDNA with a one-step gDNA removal and cDNA synthesis supermix (TransGen Biotech, Beijing, China). qPCR was performed with 2×SYBR Green Mix (GeneStar, Beijing, China) on an ABI Prism 7500 PCR instrument (Applied Biosystems, Waltham, USA). The primer sequences used for qPCR are listed in Table S1.

Accession numbers

Sequence data referred to in this article can be found in Rice Genome Annotation Project under the following accession numbers: *OsPUB73*, LOC_Os02g28870; *OsVQ25*, LOC_Os06g45570; *OsWRKY53*, LOC_Os05g27730.

QUANTIFICATION AND STATISTICAL ANALYSIS

Data for quantification analyses are presented as mean ± standard error of mean (SEM). At least two independent biological replicates were performed for each experiment. The asterisks indicate significant differences from the controls by two-tailed Student's *t*-test (*$p < 0.05$, **$p < 0.01$). The details are included in the figure legends.

Cell Reports, Volume *40*

Supplemental information

A VQ-motif-containing protein fine-tunes rice immunity and growth by a hierarchical regulatory mechanism

Zeyun Hao, Jinfu Tian, Hong Fang, Liang Fang, Xiao Xu, Feng He, Shaoya Li, Wenya Xie, Qiang Du, Xiaoman You, Debao Wang, Qiuhong Chen, Ruyi Wang, Shimin Zuo, Meng Yuan, Guo-Liang Wang, Lanqin Xia, and Yuese Ning

A

Target-base editing types of *OsPUB73* CRSPR/Cas9 lines	
5’—CCACGAGGTCTGACTACGCCGCG—3’	WT
5’—CCACAGAGGTCTGACTACGCCGCG—3’	3-1 (+A, homo)
5’—CC - GCG—3’	4-1 (-20, homo)

B

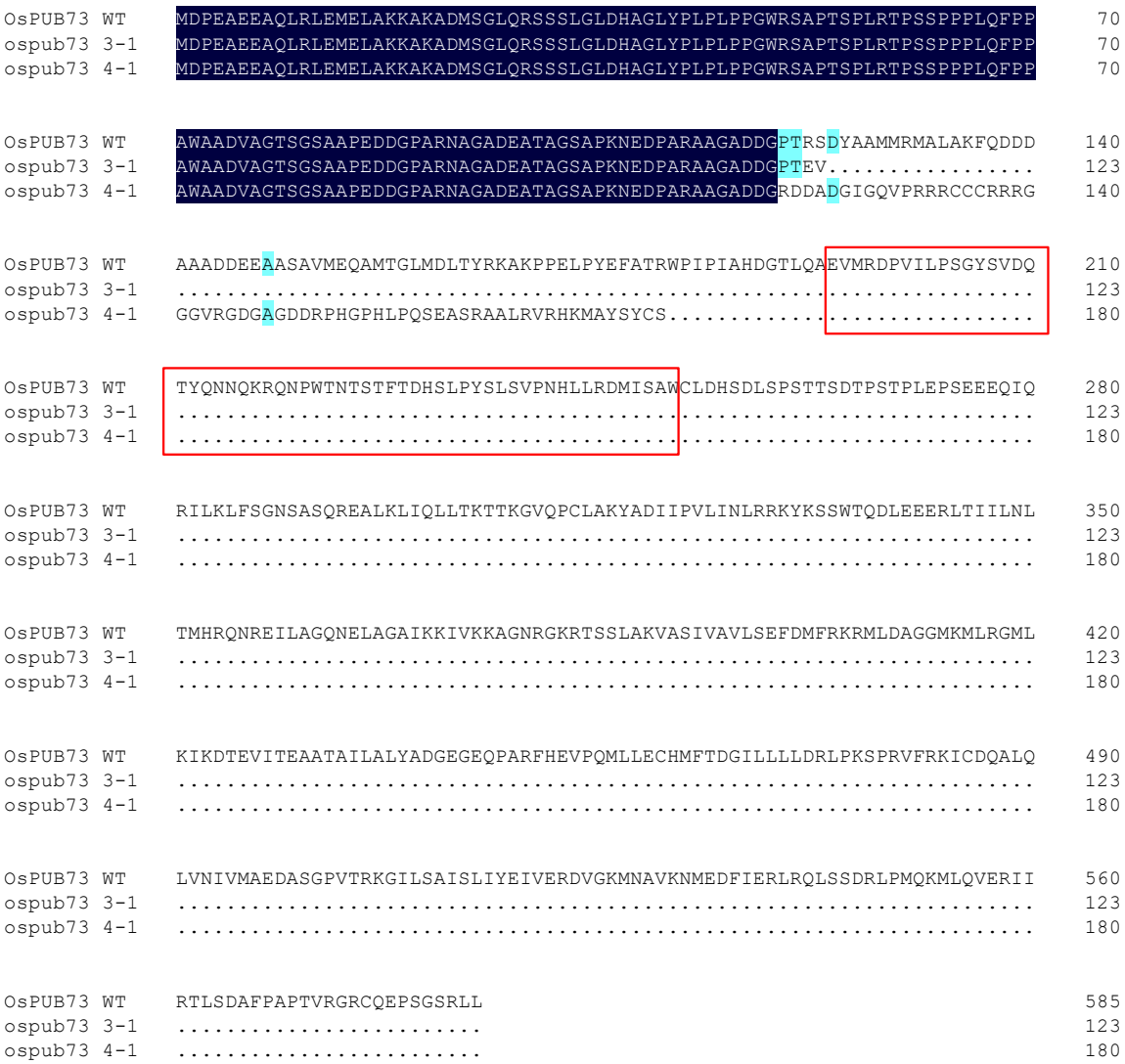

Figure S1. Analysis of *OsPUB73* CRISPR/Cas9 lines. Related to Figure 1.

(A) Sequence of the WT and *ospub73* mutant alleles, based on PCR amplification and Sanger sequencing of *OsPUB73* genomic DNA.

(B) Predicted protein sequence for OsPUB73 in WT and *ospub73* mutants. Black shading indicates shared amino acids, red boxes indicate the U-box domain of OsPUB73, and black dots indicate missing amino acids.

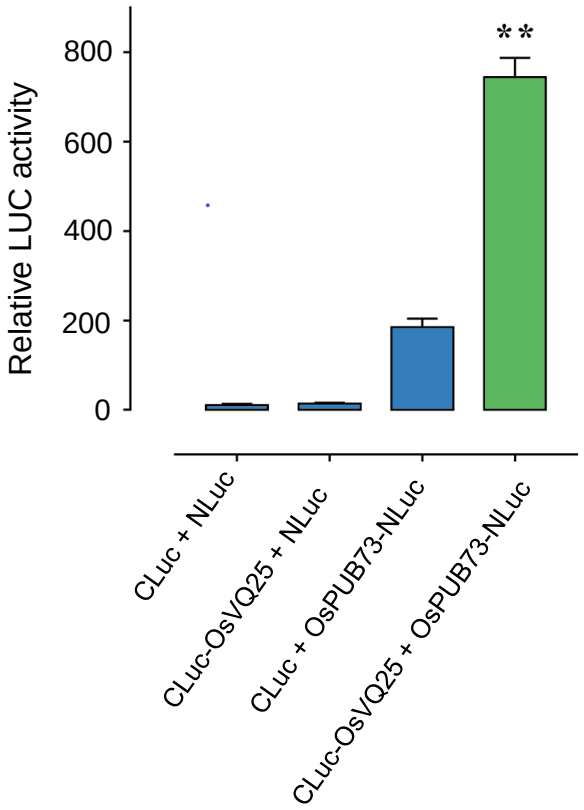

Figure S2. OsPUB73 interacts with OsVQ25 *in planta*. Related to Figure 2.

Quantitative luciferase complementation imaging assay to test the interaction between OsVQ25 and OsPUB73 in *N. benthamiana* leaves; data are shown as means ± SEM of three biological replicates. Asterisks represent statistical significance (**$P \leq 0.01$, Student's t-test).

A

Target-base editing types of *OsVQ25* CRISPR/Cas9 lines	
5’— GAGTGACACTGGCTCGAGCTTGGCG—3’	WT
5’— GAGTGACACTGGCTCGAAGCTTGGCG—3’	28-1 (+A, homo)
5’— GAGTGACACTGGCTCGACGCTTGGCG—3’	29-1 (+C, homo)
5’— GAGTGACACTGGCTCGATGCTTGGCG—3’	48-1 (+T, homo)

B

```
OsVQ25 WT      MAAMSDTGSSLAQWAELYHDASAAHGGVVANGAAAAATSPASPAGSTGGSPTRAPGVEGPRVGKPARRRS     70
osvq25 28-1    MAAMSDTGSKLGAVGRAVPRRVGCSRRRGGERCGGGGDEPGVAGGIDRREPDAGAGGGGAARGEAG...E     67
osvq25 29-1    MAAMSDTGSTLGAVGRAVPRRVGCSRRRGGERCGGGGDEPGVAGGIDRREPDAGAGGGGAARGEAG...E     67
osvq25 48-1    MAAMSDTGSMLGAVGRAVPRRVGCSRRRGGERCGGGGDEPGVAGGIDRREPDAGAGGGGAARGEAG...E     67

OsVQ25 WT      RASRRAPVTLLNTDTTNFRAMVQQFTGIPAPPAGAFAGPGGVPVINFGSDYGFTGAVLPFSDHLQPRRPT    140
osvq25 28-1    EAVQGVAARARDAAQHGHHQLPRHGAAVHRHPGAARGRVRGARRRSGHQLRLRLRLHRRRPSLLRP..PP    135
osvq25 29-1    EAVQGVAARARDAAQHGHHQLPRHGAAVHRHPGAARGRVRGARRRSGHQLRLRLRLHRRRPSLLRP..PP    135
osvq25 48-1    EAVQGVAARARDAAQHGHHQLPRHGAAVHRHPGAARGRVRGARRRSGHQLRLRLRLHRRRPSLLRP..PP    135

OsVQ25 WT      FQDHQQLLRPQQQYTGAPFGYGNLQQAGGAGTGAGDMFSHALSSAEDRLLLQSLQSAQMPTSAANHSANG    210
osvq25 28-1    TAPADVPGPPTAPPTAAAVHRRTVRLRQPAASRRRRHRRRRHVQPRAELGRGQVAPAEPPVSSDAYFRR.    204
osvq25 29-1    TAPADVPGPPTAPPTAAAVHRRTVRLRQPAASRRRRHRRRRHVQPRAELGRGQVAPAEPPVSSDAYFRR.    204
osvq25 48-1    TAPADVPGPPTAPPTAAAVHRRTVRLRQPAASRRRRHRRRRHVQPRAELGRGQVAPAEPPVSSDAYFRR.    204

OsVQ25 WT      YF                                                                        212
osvq25 28-1    ..                                                                        204
osvq25 29-1    ..                                                                        204
osvq25 48-1    ..                                                                        204
```

C

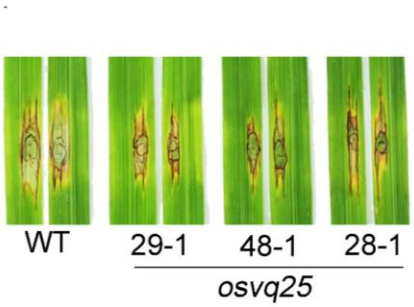

D

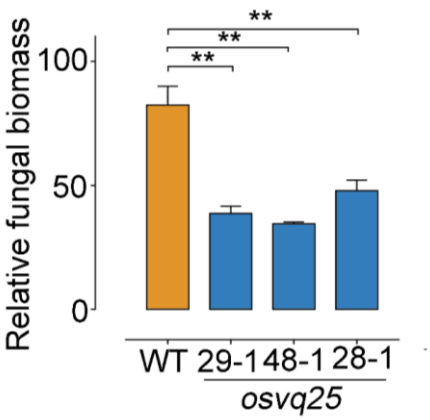

E

F

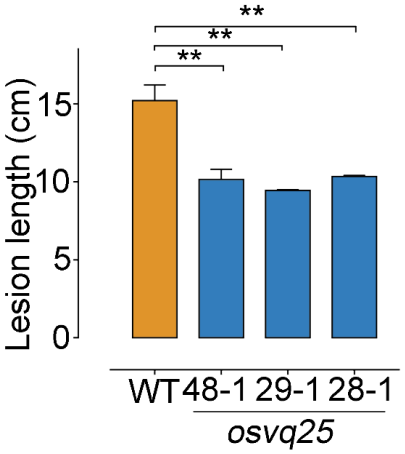

Figure S3. Loss of OsVQ25 function enhances resistance against *M. oryzae* and *Xoo*. Related to Figure 3.

(A) Sequence of the WT and *osvq25* mutant alleles, based on PCR amplification and Sanger sequencing of *OsVQ25* genomic DNA.

(B) Predicted protein sequence of OsVQ25 in WT and *osvq25* mutants. Black shading indicates shared amino acids, pink shading indicates amino acids not present in the WT sequence, red box indicates the VQ domain of OsVQ25, and black dots indicate missing amino acids.

(C) Phenotypes of the leaves from eight-week-old *osvq25* mutant plants inoculated with the compatible *M. oryzae* isolate RO1-1.

(D) Relative fungal biomass, as determined by qPCR $^{[2[CT(OsUbq)\text{-}CT(MoPot2)]]}$; data are shown as means ± SEM (n = 3 biological replicates).

(E) Phenotypes of the leaves from eight-week-old *osvq25* mutant plants inoculated with the *Xoo* isolate PXO86 .

(F) Lesion length in WT and *osvq25* mutants inoculated with the *Xoo* isolate PXO86; data are shown as means ± SEM (n = 3 biological replicates).

Asterisks in (D) and (F) represent statistical significance (**$P \leq 0.01$, Student's t-test).

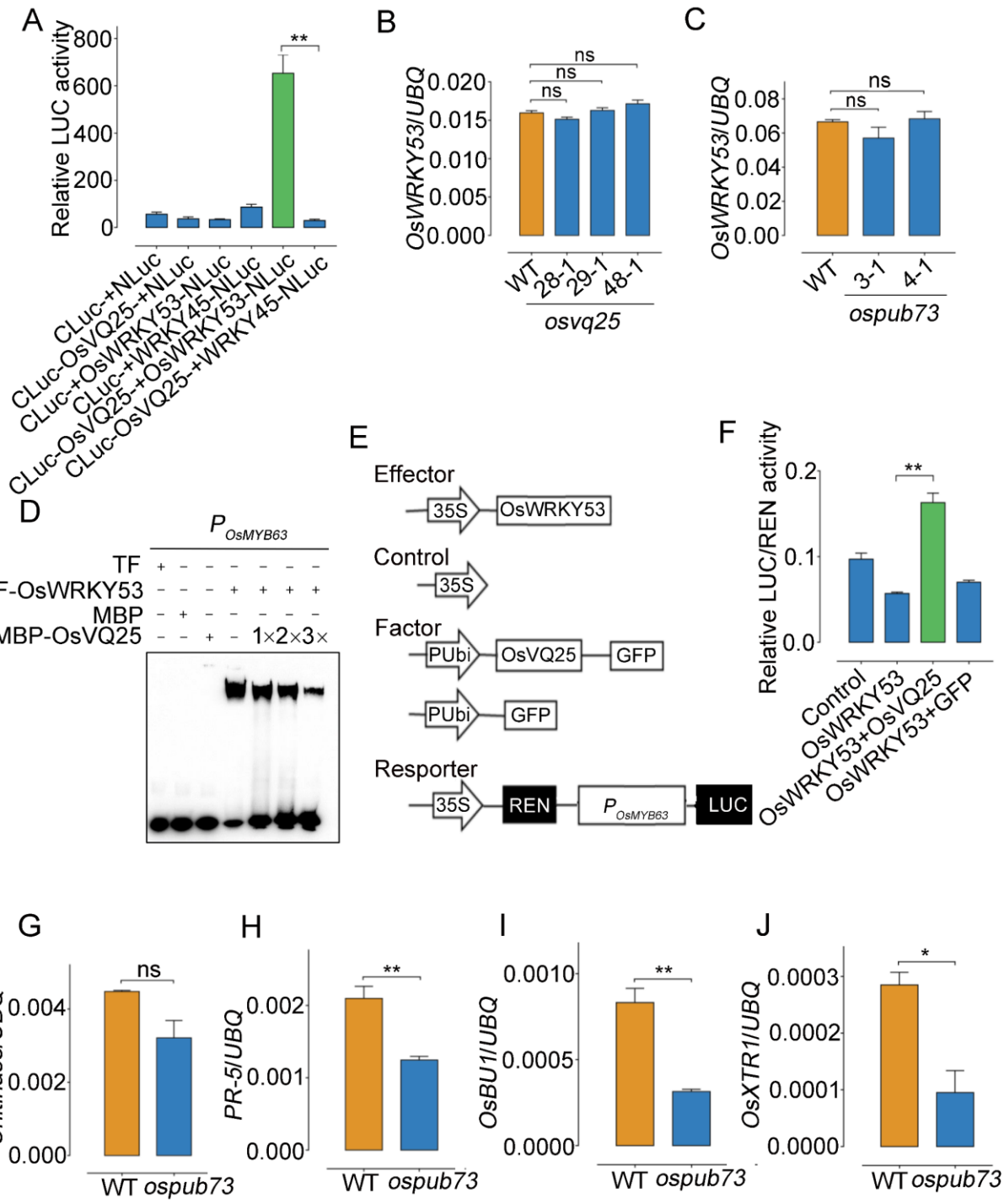
A
Relative LUC activity
800
600
400
200
0
**
CLuc-+NLuc
CLuc-OsVQ25-+NLuc
CLuc-+OsWRKY53-NLuc
CLuc-+WRKY45-NLuc
CLuc-OsVQ25-+OsWRKY53-NLuc
CLuc-OsVQ25-+WRKY45-NLuc
B
OsWRKY53/UBQ
0.020
0.015
0.010
0.005
0.000
ns
ns
ns
WT
28-1
29-1
48-1
osvq25
C
OsWRKY53/UBQ
0.08
0.06
0.04
0.02
0.00
ns
ns
WT
3-1
4-1
ospub73
D
P OsMYB63
TF
TF-OsWRKY53
MBP
MBP-OsVQ25
1×2×3×
E
Effector
35S
OsWRKY53
Control
35S
Factor
PUbi
OsVQ25
GFP
PUbi
GFP
Resporter
35S
REN
P OsMYB63
LUC
F
Relative LUC/REN activity
0.2
0.1
0.0
**
Control
OsWRKY53
OsWRKY53+OsVQ25
OsWRKY53+GFP
G
Chitinase/UBQ
0.004
0.002
0.000
ns
WT
ospub73
H
PR-5/UBQ
0.002
0.001
0.000
**
WT
ospub73
I
OsBU1/UBQ
0.0010
0.0005
0.0000
**
WT
ospub73
J
OsXTR1/UBQ
0.0003
0.0002
0.0001
0.0000
*
WT
ospub73

Figure S4. OsVQ25 interacts with OsWRKY53 and suppresses the transcriptional activity and DNA binding of OsWRKY53. Related to Figure 5.

(A) Quantitative luciferase complementation imagine assay to test the interaction between OsVQ25 and OsWRKY53 in *N. benthamiana* leaves. Data are shown as means ± SEM (n = 3 biological replicates).

(B) Relative *OsWRKY53* transcript levels in *osvq25* mutants and WT plants, as determined by qRT-PCR. Rice *UBIQUITIN* (*UBQ*) was used as the reference gene to normalize gene expression. Data are shown as means ± SEM (n = 3 biological replicates).

(C) Relative *OsWRKY53* transcript levels in *ospub73* mutants and WT plants, as determined by qRT-PCR. Rice *UBIQUITIN* (*UBQ*) was used as the reference gene to normalize gene expression.

(D) OsVQ25 inhibits OsWRKY53 binding to the *OsMYB63* promoter in EMSA. '1×', '2×', and '3×' indicate the addition of 10 μg, 20 μg, or 30 μg recombinant purified MBP-OsVQ25 in the EMSA, respectively.

(E) Constructs used in dual-luciferase assay of OsWRKY53 in regulating *OsMYB63* expression.

(F) OsVQ25 increases *OsMYB63* expression in the dual-luciferase assay. The *ProOsMYB63:LUC* reporter construct was co-transfected with control, or with the constructs *35S:OsWRKY53*, *35S:OsWRKY53 + Ubi:OsVQ25*, or *35S:OsWRKY53 + Ubi:GFP* in rice protoplasts respectively. LUC and REN activity was determined at 24 h after transformation. Values are means ± SEM (n = 3 biological replicates).

(G-H) Expression of the OsWRKY53 downstream defense-related genes *Chitinase* and *PR-5* in *ospub73* mutants and WT plants, as determined by qRT-PCR. Rice *UBIQUITIN* (*UBQ*) was used as the reference gene to normalize gene expression. Data are shown as means ± SEM (n = 3 biological replicates).

(I-J) Relative transcript levels of the OsWRKY53 downstream BR-signaling genes *OsBU1* (C) and *OsXTR1* (D) in *ospub73* mutants and WT plants, as determined by qRT-PCR. Data are shown as means ± SEM (n = 3 biological replicates).

For (A)-(C), (F)-(J), 'ns' indicates no statistical significance at $p > 0.05$, asterisks represent statistical significance, *$P \leq 0.05$, **$P \leq 0.01$, Student's t-test.

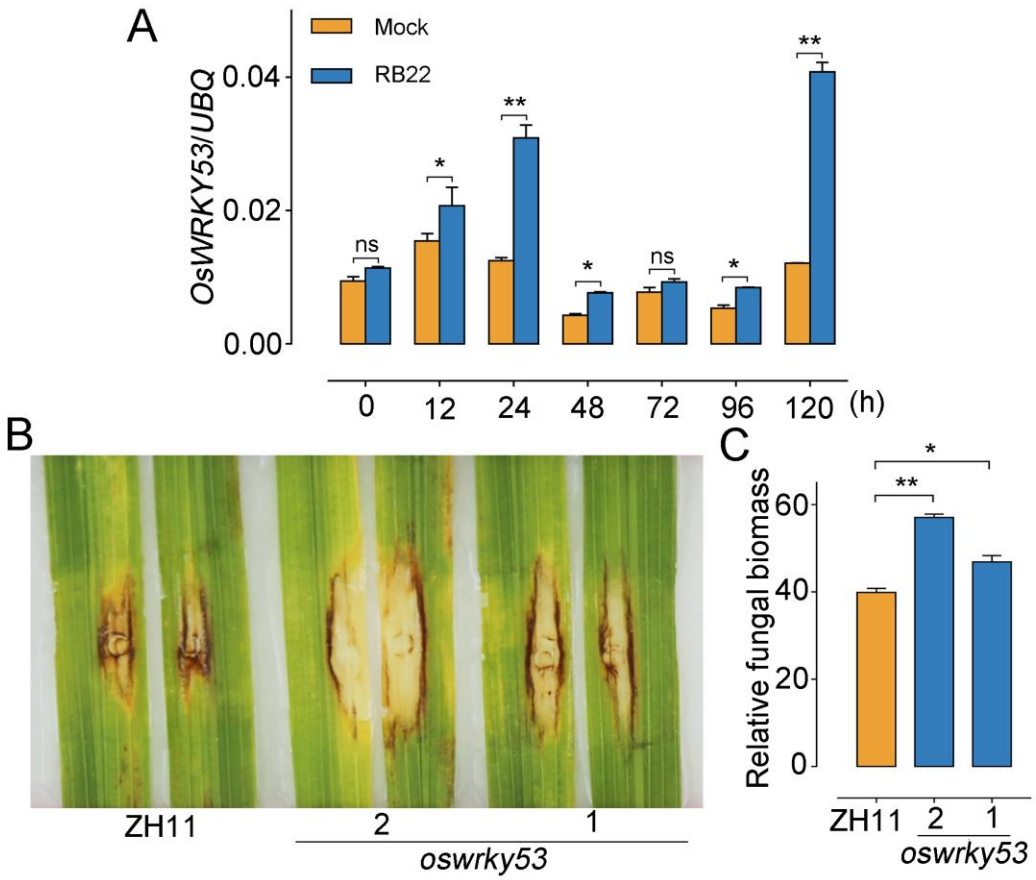

Figure S5. Loss of OsWRKY53 function suppresses *M. oryzae* resistance. Related to Figure 5.

(A) Relative *OsWRKY53* transcript levels in NPB plants inoculated with the compatible *M. oryzae* isolate RB22, as determined by qRT-PCR. We used ddH_2O containing 0.1% (v/v) Tween 20 as the mock-inoculation control and rice *UBIQUITIN* (*UBQ*) as the reference gene to normalize gene expression. Values are means ± SEM of two biological replicates.

(B) Phenotypes of the leaves from eight-week-old *oswrky53* mutant plants inoculated with the compatible *M. oryzae* isolate RB22.

(C) Relative fungal biomass as determined by qPCR [$2^{[CT(OsUbq)-CT(MoPot2)]}$]; data are shown as means ± SEM (n = 3 biological replicates).

For (A) and (C), 'ns' indicates no statistical significance at $p > 0.05$, asterisks represent statistical significance, *$P \leq 0.05$, **$P \leq 0.01$, Student's t-test.

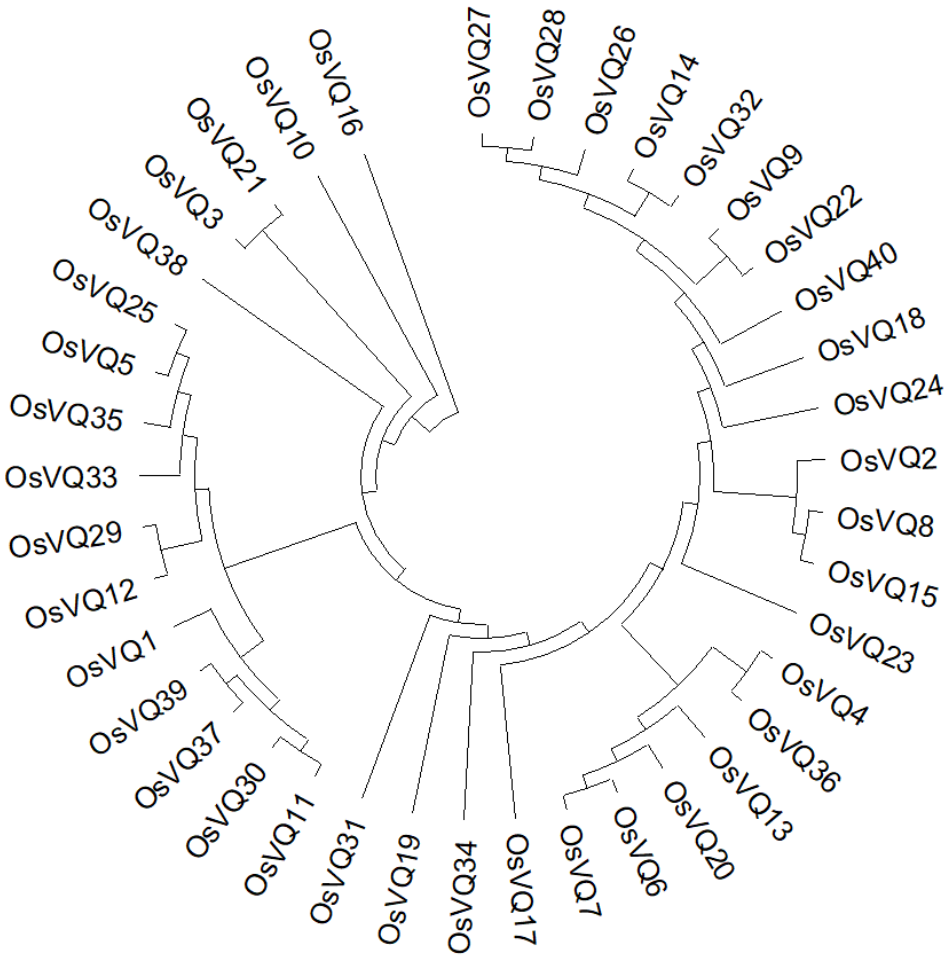

Figure S6. Phylogenic tree of VQ domain proteins in rice. Related to Figure 6.
The full-length amino acid sequences of the 40 VQ proteins in rice were aligned by ClustalW, from which a phylogenic tree of VQ proteins was constructed, using the neighbor-joining method with 1,000 bootstrap replicates.

Table S1. Primers used in the paper. Related to STAR Methods.

Primer Name	Primer Sequence （5'-3'）
Plasmid construction	
Knockout	
OsVQ25-CRISPR-Forward	GGCAGGCGCGTCGCGAAGCCCGCG
OsVQ25-CRISPR-Reverse	AAACCGCGGGCTTCGCGACGCGCC
OsPUB73-CRISPR-Forward	GCCGCGCCGATGATGGCCCCACG
OsPUB73-CRISPR-Reverse	AAACCGCGGCGTAGTCAGACCTCG
Luciferase complementation	
pCLuc-OsVQ25-Forward	GCGTCCCGGGGCGGTACCATGGCGGCCATGAGTGACAC
pCLuc-OsVQ25-Reverse	AAAGCTCTGCAGGTCGACGGCGAAGTAACCATTAGCGC
pNLuc-OsPUB73-Forward	GGGGACGAGCTCGGTACCATGGATCCGGAGGCGGAGGA
pNLuc-OsPUB73-Reverse	GTACGAGATCTGGTCGACAGCTAGAAGACGGCTTCCAC
pNLuc-OsWRKY53-Forward	GGGGACGAGCTCGGTACCATGGCGTCCTCGACGGGGGGGT
pNLuc-OsWRKY53-Reverse	GTACGAGATCTGGTCGACGCAGAGGAGCGACTCGACGAAC
pNLuc-WRKY45-Forward	GGGGACGAGCTCGGTACCATGACGTCATCGATGTCGCCG
pNLuc-WRKY45-Reverse	GTACGAGATCTGGTCGACAAAGCTCAAACCCATAATGTC
Co-immunoprecipitation and degradation assay	
pRTVcGFP-OsVQ25-Forward	CCAGATCCAGTGGGATCCATGGCGGCCATGAGTGACACTG
pRTVcGFP-OsVQ25-Reverse	GGCCGCACTAGTAAGCTTGGCGAAGTAACCATTAGCGCT
pRTVcHA-OsPUB73-Forward	GATCCAGTGGGATCCATGGATCCGGAGGCGGAGGA
pRTVcHA-OsPUB73-Reverse	CGCACTAGTAAGCTTAGCTAGAAGACGGCTTCCAC
pRTVcHA-OsPUB73-C-Forward	GGATCCCCGGGTGAGCTCATGTCCCCATCTACCACTTCTGA
pRTVcHA-OsWRKY53-Forward	CCAGATCCAGTGGGATCCATGGCGTCCTCGACGGGGGGG
pRTVcHA-OsWRKY53-Reverse	AGCGGCCGCACTAGTAAGCTTGCAGAGGAGCGACTCGACGAA
pRTVcHA-WRKY45-Forward	CCAGATCCAGTGGGATCCATGACGTCATCGATGTCGCCG
pRTVcHA-WRKY45 -Reverse	AGCGGCCGCACTAGTAAGCTTAAAGCTCAAACCCATAATGTC
BiFC assay	
p2YN-OsVQ25-Forward	CATTTACGAACGATAGTTAATTAAATGGCGGCCATGAGTGACAC
P2YN-OsVQ25-Reverse	CACTGCCACCTCCTCCACTAGTGGCGAAGTAACCATTAGCGC
p2YC-PUB73-Forward	CATTTACGAACGATAGTTAATTAAATGGATCCGGAGGCGGAGGA
p2YC-PUB73-Reverse	CACTGCCACCTCCTCCACTAGTAGCTAGAAGACGGCTTCCAC
p2YC-OsWRKY53-Forward	CATTTACGAACGATAGTTAATTAAATGGCGTCCTCGACGGGGGGGT
p2YC-OsWRKY53-Reverse	CACTGCCACCTCCTCCACTAGTGCAGAGGAGCGACTCGACGAAC
p2YC-WRKY45- Forward	CATTTACGAACGATAGTTAATTAAATGACGTCATCGATGTCGCCG
p2YC-WRKY45- Reverse	CGACTCTAGAGGATCCTCAGGAGGGGTAAGAAGCCTT
Transcriptional activity assay	
pGreenII62-OsVQ25-Forward	TCCCCGGGATGGCGGCCATGAGTGACACTG
pGreenII62-OsVQ25-Reverse	CGGTCGACCTAGGCGAAGTAACCATTAGCG
GAL4DB-OsWRKY53-Forward	TCCCCCGGGGATGGCGTCCTCGACGGGGGGGT
GAL4DB-OsWRKY53-Reverse	CGGTCGACCTAGCAGAGGAGCGACTCGACGA
qRT-PCR	
Gene expression	
Q-OsPUB73-Forward	ATTTCATCGAGCGGTTGCGT

Q-OsPUB73-Rreverse	CTCCAGAAAGTTAAGCGAGCA
Q-OsVQ25-Forward	CCTCCAGTCAGCTCAGAT
Q-OsVQ25-Reverse	AACACAACTGGTCCATGAAT
Q-OsWRKY53-Forward	GAGCGACATCGACATCCT
Q-OsWRKY53-Reverse	TTGTGCTTGCCCTCGTAG
Q-OsPBZ1-Forward	TGGCATGCTCAAGATGATCGAGGA
Q-OsPBZ1-Reverse	TTACTCTCACGGACTCAAACGCCA
Q-OsPR1-Forward	CTGGTGGAGGGCGGCGGCAT
Q-OsPR1-Reverse	CCGGCTCGCCGGCGACCAT
Q-WRKY45-Forward	CGGGTAAAACGATCGAAAGA
Q-WRKY45-Reverse	GACCCCCAGCTCATAATCAA
Q-Chitinase-Forward	GCTACGCCTACGAACCATTC
Q-Chitinase-Reverse	GTCCGGTCGGTGTACATTCT
Q-PR-5-Forward	GCATTAGCTGGCTGCTATAGAT
Q-PR-5-Reverse	CCATGGACGATTATTATCTTATTATTT
Q-OsBU1-Forward	ATCTCCAAGCTCCAGTCCCT
Q-OsBU1-Reverse	GCTCTTGATGTAGCTGCACG
Q-OsXTR1-Forward	GGAGCCGTACATCCTGCAGA
Q-OsXTR1-Reverse	AGGCTGGAGTAGAGCTTCATCG
Q-UBQ-Forward	CGCAAGAAGAAGTGTGGTCA
Q-UBQ-Reverse	GGGAGATAACAACGGAAGCA
Fungal biomass determination	
Q-MoPot2-Forward	ACGACCCGTCTTTACTTATTTGG
Q-MoPot2-Reverse	AAGTAGCGTTGGTTTTGTTGGAT
Q-OsUbq-Forward	TTCTGGTCCTTCCACTTTCAG
Q-OsUbq-Reverse	ACGATTGATTTAACCAGTCCATGA
RT-PCR	
RT-OsVQ25-Forward	TCAACACGGACACCACCAAC
RT-OsVQ25-Reverse	GTGGTTAGCGGCGGAAGTAG
RT-Actin-Forward	TGCTATGTACGTCGCCATCCAG
RT-Actin-Reverse	TGACGGAGCGTGGTTACTCATT
Mutant identification	
OsVQ25-Identify-Forward	GATGTCATGATCGGACGGCT
OsVQ25-Identify-Reverse	ACACGGACACCACCAACTT
OsPUB73-Identify-Forward	GCTTGTATCCGCTGCCATTGC
OsPUB73-Identify-Reverse	CTAAAACAAACAGGAACAAAG